USER MANUAL FOR COMCOT VERSION 1.7
(FIRST DRAFT)

by

Xiaoming Wang

Febury 2009

ACKNOWLEDGEMENTS

TABLE OF CONTENTS

LIST OF TABLES

LIST OF FIGURES

CHAPTER 1

INTRODUCTION

Tsunami is a typical long wave in the ocean, generated by seafloor or water surface disturbances over a sufficiently large area. It has been observed and recorded since ancient times, especially in Japan and the Mediterranean areas. The earliest recorded tsunami occurred in $2,000$ B.C. off the coast of Syria (Lander and Lockridge, 1989). In recent years, the most devastating tsunami was triggered by the 2004 Sumatra earthquake off the coast of Indonesia and caused tremendous property loss and over $225,000$ casualties in the surrounding countries of Indian Ocean, especially in Indonesia, Sri Lanka, Thailand and India.

For the tsunami hazard mitigation, it is very important to construct inundation maps along those coastlines vulnerable to tsunami flooding. These maps should be developed based on the historical tsunami events and hypothetical scenarios. To produce realistic and reliable inundation estimates, it is essential to use a numerical model that calculates accurately the tsunami propagation from a source region to the coastal areas of concern and the subsequent tsunami run-up and inundation.

In many events, the wavelength of a tsunami is usually long compared to the water depth, the dispersion effect, measured by $\mu = h_0/l_0$, can be practically neglected if h_0/l_0 is smaller than 1/20. In this scenario, shallow water equations are adequate for studying tsunami evolutions. Numerical models based on shallow water equations are generally very efficient in simulating transoceanic tsunamis due to the use of explicit numerical schemes and no need to solve higher-order derivatives associated with non-linearity and frequency dispersion. COMCOT is one of the models based on Shallow Water Equations.

COMCOT (Cornell Multi-grid Coupled Tsunami model) adopts explicit staggered leap-frog finite difference schemes to solve Shallow Water Equations in both Spherical and Cartesian Coordinates. A nested grid system, dynamically coupled up to 12 levels (which will be also referred to as layers) with different grid resolution, can be implemented in the model to fulfill the need for tsunami simulations in different scales. Nested grid system means in a region of one grid size, there is one or more regions with smaller grid sizes situated in, which eventually, forms a hierarchy of grids, or grid levels. The region with largest grid size is called 1st-level grid and all the grid regions directly nested in the 1st level grid, are called 2nd-level grids, so on and so forth. In one grid region, up to 12 sub-level grid regions can be defined. It should be noted that in one grid region, a uniform grid size ($\triangle x = \triangle y$) is adopted in COMCOT. Spherical or Cartesian coordinate system, as well as either linear or nonlinear version of governing equations can be chosen for each region. The water surface displacement is assumed the same as the deformation of the sea floor as long as the uplift motion is much faster than the wave propagation; otherwise, submarine landslide model should be used to include transient effect. For a given earthquake, the displacement of seafloor is determined from a linear elastic dislocation theory (Mansinha and Smylie, 1971; Okada, 1985).

For theoretical background and detailed derivations, please refer to Liu et al. (1998), *Computer programs for tsunami propagation and inundation*, Cornell University.

1.1 Features

COMCOT is capable of efficiently studying the entire life-span of a tsunami, including its generation, propagation, runup and inundation. Multiple tsunami-generating mechanisms can be implemented in COMCOT, including instal or transient faulting, land-

slides, water surface disturbances or wave maker. Both linear and nonlinear Shallow Water Equations are available in spherical or Cartesian coordinate system for numerical studies at different scales. Nested grid configuration balances the efficiency and accuracy in which larger grid size can be used in the open sea for studying tsunami propagation and finer grids can be adopted for coastal regions of interest. Some features are briefly listed below:

⋄ Explicit Leap-Frog finite difference scheme to solve linear and nonlinear shallow water equations in spherical and cartesian coordinates;

⋄ Nested grid configuration

⋄ Multiple tsunami-generating mechanisms, including instant faulting (Mansinha and Smylie (1971) and Okada (1985)), transient floor motion (e.g., landslides or transient faulting), water surface disturbance and wave maker;

⋄ Implementation of constant or variable bottom roughness;

⋄ Dispersion-improved numerical scheme;

⋄ Flexible input/output options

1.2 Brief History

COMCOT originated from the creation of Yongsik Cho and S.N. Seo (version 1.0) based on the theoretical and numerical work of Shuto (1991); **?** and Imamura et al. (1988). Moving boundary scheme was introduced and validated against experimental studies (Liu et al., 1995). Dr. Seung-Buhm Woo introduced a user interface (i.e., parameter file) and develop a general grid matching algorithm (1999) and finally formed

version 1.4. Many achievements were made with COMCOT during this period, such as the successful simulations of 1960 Chile Tsunami (Liu et al., 1994) and 1986 Taiwan Hua-lien tsunami, involving the modelling of tsunami generation, propagation, runup and inundation. The coming of Fortran 90 gave a new power to the programming of COMCOT. With the helps of many others, especially Tom Logan (ARSC), Steven Lantz (Cornell University) and Philip L.-F. Liu (Cornell University), further improvements and modifications were introduced by Xiaoming Wang (2003-), which yielded version 1.5 and 1.6. And subroutines dealing with nonlinear equations were also optimized to get a better efficiency by Tom Logan (ARSC, 2003). One of the significant progresses is the migration from Fortran 77 to Fortran 90, allowing dynamic allocation of arrays. The structure of COMCOT was re-organized and a new user interface and parameter modules was introduced, making the code much neat and more expandable. Most of subroutines were rewritten during this time and more tsunami-generating mechanism were implemented. A new grid-nesting algorithm was developed to allow more efficient and flexible grid setup. Numerical simulations performed on this version include 2002 Hua-lien tsunami, 2003 Algerian tsunami, 2004 and 2005 Indian Ocean tsunamis and 2006 Java tsunami. For the 2004 Giant Tsunami, both runup and inundation were extensively studied in several regions.

In version 1.7, the solver kernel is re-packaged with a more efficient interface. More data formats are supported. Moreover, the grid-matching becomes much easier. Once the region of sub-level grids is defined (by coordinates of lower-left and upper-right corners), the grid-matching is done automatically by COMCOT. In addition, a dispersion-improved algorithm is also added into the solver so that COMCOT will be able to simulate linear/weakly nonlinear dispersive waves, but still keep a high computational efficiency.

CHAPTER 2

GOVERNING EQUATIONS AND NUMERICAL METHODS

2.1 Governing Equations

Linear and nonlinear shallow water equations in both Spherical and Cartesian Coordinates are implemented in COMCOT. For tsunamis in deep ocean, tsunami amplitude is much smaller than the water depth and linear shallow water equations in Spherical Coordinates can be applied.

$$\frac{\partial \eta}{\partial t} + \frac{1}{R \cos \varphi} \left\{ \frac{\partial P}{\partial \psi} + \frac{\partial}{\partial \varphi}(\cos \varphi Q) \right\} = -\frac{\partial h}{\partial t} \tag{2.1}$$

$$\frac{\partial P}{\partial t} + \frac{gh}{R \cos \varphi} \frac{\partial \eta}{\partial \psi} - fQ = 0 \tag{2.2}$$

$$\frac{\partial Q}{\partial t} + \frac{gh}{R} \frac{\partial \eta}{\partial \varphi} + fP = 0 \tag{2.3}$$

where η is the water surface elevation; (P, Q) denote the volume fluxes in X (West-East) direction and Y (South-North) direction, respectively; (φ, ψ) denote the latitude and longitude of the Earth; R is the radius of the Earth; g is the gravitational acceleration and h is the water depth. And the term $-\frac{\partial h}{\partial t}$ reflects the effect of transient seafloor motion, can be used to model landslide-generated tsunamis. f represents the Coriolis force coefficient due to the rotation of the Earth and

$$f = \Omega \sin \varphi \tag{2.4}$$

and Ω is the rotation rate of the Earth.

When a simulation involving a relatively small region in which the Earth rotation effect is not prominent, shallow water equations in Cartesian Coordinates are preferred. The follow linear shallow water equations in Cartesian Coordinates are also imple-

mented in COMCOT.

$$\frac{\partial \eta}{\partial t} + \left\{ \frac{\partial P}{\partial x} + \frac{\partial Q}{\partial y} \right\} = -\frac{\partial h}{\partial t} \tag{2.5}$$

$$\frac{\partial P}{\partial t} + gh\frac{\partial \eta}{\partial x} - fQ = 0 \tag{2.6}$$

$$\frac{\partial Q}{\partial t} + gh\frac{\partial \eta}{\partial y} + fP = 0 \tag{2.7}$$

where (P, Q) denote the volume fluxes in X (West-East) direction and Y (South-North) direction, respectively, and both are products of velocity and water depth, i.e., $P = hu$ and $Q = hv$.

Since as the tsunami propagates over a continental shelf and approaches a coastal area, linear shallow water equations are no longer valid. The wave length of the incident tsunami becomes shorter and the amplitude becomes larger as the leading wave of a tsunami propagates into shallow water. Therefore, the nonlinear convective inertia force and bottom friction terms become increasingly important, while the significance of the Coriolis force and the frequency dispersion terms diminishes. The nonlinear shallow water equations including bottom friction effects are adequate to describe the flow motion in the coastal zone (Kajiura and Shuto, 1990; Liu et al., 1994). Furthermore, along the shoreline, where the water depth becomes zero, a special treatment is required to properly track shoreline movements.

In COMCOT, the following nonlinear shallow water equations are implemented in Spherical Coordinates as

$$\frac{\partial \eta}{\partial t} + \frac{1}{R\cos\varphi} \left\{ \frac{\partial P}{\partial \psi} + \frac{\partial}{\partial \varphi}(\cos\varphi Q) \right\} = -\frac{\partial h}{\partial t} \tag{2.8}$$

$$\frac{\partial P}{\partial t} + \frac{1}{R\cos\varphi}\frac{\partial}{\partial \psi}\left\{ \frac{P^2}{H} \right\} + \frac{1}{R}\frac{\partial}{\partial \varphi}\left\{ \frac{PQ}{H} \right\} + \frac{gH}{R\cos\varphi}\frac{\partial \eta}{\partial \psi} - fQ + F_x = 0 \tag{2.9}$$

$$\frac{\partial Q}{\partial t} + \frac{1}{R\cos\varphi}\frac{\partial}{\partial \psi}\left\{ \frac{PQ}{H} \right\} + \frac{1}{R}\frac{\partial}{\partial \varphi}\left\{ \frac{Q^2}{H} \right\} + \frac{gH}{R}\frac{\partial \eta}{\partial \varphi} + fP + F_y = 0 \tag{2.10}$$

and in Cartesian Coordinates as

$$\frac{\partial \eta}{\partial t} + \left\{ \frac{\partial P}{\partial x} + \frac{\partial Q}{\partial y} \right\} = -\frac{\partial h}{\partial t} \tag{2.11}$$

$$\frac{\partial P}{\partial t} + \frac{\partial}{\partial x} \left\{ \frac{P^2}{H} \right\} + \frac{\partial}{\partial y} \left\{ \frac{PQ}{H} \right\} + gH\frac{\partial \eta}{\partial x} + F_x = 0 \tag{2.12}$$

$$\frac{\partial Q}{\partial t} + \frac{\partial}{\partial x} \left\{ \frac{PQ}{H} \right\} + \frac{\partial}{\partial y} \left\{ \frac{Q^2}{H} \right\} + gH\frac{\partial \eta}{\partial y} + F_y = 0 \tag{2.13}$$

in which H is the total water depth and $H = \eta + h$; F_x and F_y represents the bottom friction in X and Y directions, respectively. And these two terms are evaluated via Manning's formula

$$F_x = \frac{gn^2}{H^{7/3}}P(P^2 + Q^2)^{1/2} \tag{2.14}$$

$$F_x = \frac{gn^2}{H^{7/3}}Q(P^2 + Q^2)^{1/2} \tag{2.15}$$

where n is the Manning's roughness coefficient.

2.2   Numerical Method

Explicit leap-frog finite difference method is adopted to solve both linear and nonlinear shallow water equations (Cho, 1995). The evaluation of water surface elevation, η, and volume fluxes, P and Q, are staggered in time and space. Figure 2.1 shows a grid system in which the water surface displacement η is evaluated at the center of a grid cell and volume fluxes P and Q (product of velocity and water depth) are evaluated at edge centers (i.e., $(i + 1/2, j)$ and $(i, j + 1/2)$) of the grid cell.

The numerical scheme has a truncation error of $O(\triangle x^2, \triangle y^2, \triangle t^2)$. The explicit leap-frog finite difference scheme for linear shallow water equations can be expressed as

$$\frac{\eta_{i,j}^{n+1/2} - \eta_{i,j}^{n-1/2}}{\triangle t} + \left\{ \frac{1}{R\cos\varphi} \right\}_{i,j} \frac{P_{i+1/2,j}^n - P_{i-1/2,j}^n}{\triangle \psi} \tag{2.16}$$
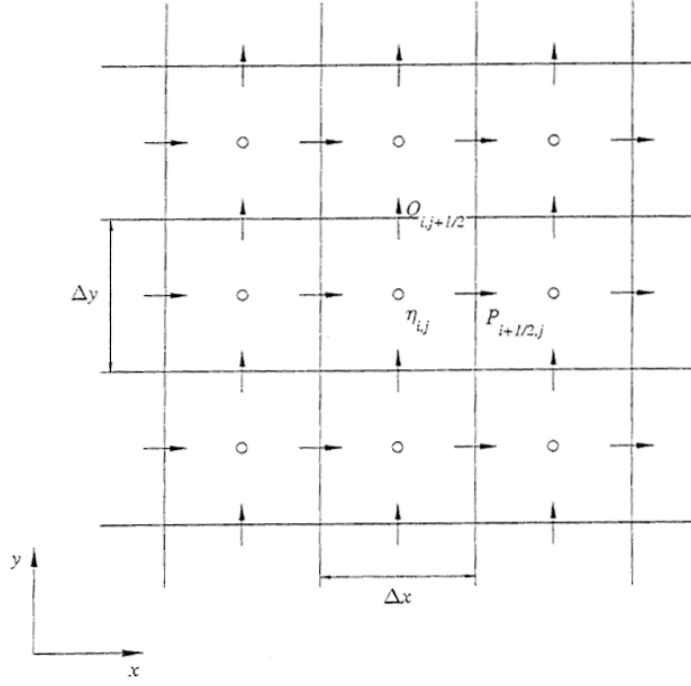
Figure 2.1: Sketch of Staggered Grid Setup in COMCOT.

$$+\left\{\frac{1}{R\cos\varphi}\right\}_{i,j}\frac{(\cos\varphi_{i,j+1/2})Q^n_{i,j+1/2}-(\cos\varphi_{i,j-1/2})Q^n_{i,j-1/2}}{\Delta\varphi}=-\frac{h^{n+1/2}_{i,j}-h^{n-1/2}_{i,j}}{\Delta t} \quad (2.17)$$

$$\frac{P^{n+1}_{i+1/2,j}-P^n_{i+1/2,j}}{\Delta t}+\left\{\frac{gh}{R\cos\varphi}\right\}_{i+1/2,j}\frac{\eta^{n+1/2}_{i+1,j}-\eta^{n+1/2}_{i,j}}{\Delta\psi}-fQ^n_{i+1/2,j}=0 \quad (2.18)$$

$$\frac{Q^{n+1}_{i,j+1/2}-Q^n_{i,j+1/2}}{\Delta t}+\left\{\frac{gh}{R}\right\}_{i,j+1/2}\frac{\eta^{n+1/2}_{i,j+1}-\eta^{n+1/2}_{i,j}}{\Delta\varphi}+fQ^n_{i,j+1/2}=0 \quad (2.19)$$

in Spherical Coordinates for a large scale simulation and

$$\frac{\eta^{n+1/2}_{i,j}-\eta^{n-1/2}_{i,j}}{\Delta t}+\frac{P^n_{i+1/2,j}-P^n_{i-1/2,j}}{\Delta x}+\frac{Q^n_{i,j+1/2}-Q^n_{i,j-1/2}}{\Delta y}=-\frac{h^{n+1/2}_{i,j}-h^{n-1/2}_{i,j}}{\Delta t} \quad (2.20)$$

$$\frac{P^{n+1}_{i+1/2,j}-P^n_{i+1/2,j}}{\Delta t}+gh_{i+1/2,j}\frac{\eta^{n+1/2}_{i+1,j}-\eta^{n+1/2}_{i,j}}{\Delta x}=0 \quad (2.21)$$

$$\frac{Q^{n+1}_{i,j+1/2}-Q^n_{i,j+1/2}}{\Delta t}+gh_{i,j+1/2}\frac{\eta^{n+1/2}_{i,j+1}-\eta^{n+1/2}_{i,j}}{\Delta y}=0 \quad (2.22)$$

in Cartesian Coordinates for a small scale simulation.

From the continuity equation, the proposed leap-frog scheme calculates the free sur-

8

face elevation at the $(i, j) - th$ grid point on the $(n + 1/2) - th$ time step. These computations are fully explicit and require information on the volume flux components and the free surface displacement from the previous time step. The volume flux components are not evaluated at the same location as that for the free surface displacement. Figure ?? shows a grid system in which the free surface displacement, η, is calculated at the center of a grid cell (i, j) and the volume flux components, P and Q, are obtained at the centers of four edges of the grid cell, i.e., $P_{i-1/2,j}$, $P_{i+1/2,j}$, $Q_{i,j-1/2}$ and $Q_{i,j+1/2}$. The momentum equations, ?? and ??, are then used to calculate the volume flux components, $P_{i+1/2,j}$ and $Q_{i,j+1/2}$. Note that the calculations for the free surface displacement and the volume flux components are also staggered in time.

The nonlinear shallow water equations are discretized by using the same leap-frog finite difference scheme as the linear shallow water equations. The nonlinear convection terms are discretized with an upwind scheme. In general, the upwind scheme is conditionally stable and introduces some numerical dissipation. But if the velocity gradient in the fluid field is not too large and if the stability condition, which is $\sqrt{gh}\triangle t/\triangle x < 1$ is satisfied, upwind formulation is preferred for solving advective terms since, at each time step, only a small computational effort is required. The free surface elevation is evaluated at time levels $t = (n - 1/2)\triangle t$ and $t = (n + 1/2)\triangle t$ however the volume flux components are calculated at time levels $t = n\triangle t$ and $t = (n + 1)\triangle t$.

The nonlinear convective terms in the momentum equations in Cartesian coordinate system are discretized by using an upwind scheme and given as

$$\frac{\partial}{\partial x}\left\{\frac{P^2}{H}\right\} = \frac{1}{\triangle x}\left\{\lambda_{11}\frac{(P_{i+3/2,j}^n)^2}{H_{i+3/2,j}^n} + \lambda_{12}\frac{(P_{i+1/2,j}^n)^2}{H_{i+1/2,j}^n} + \lambda_{13}\frac{(P_{i-1/2,j}^n)^2}{H_{i-1/2,j}^n}\right\} \quad (2.23)$$

$$\frac{\partial}{\partial y}\left\{\frac{PQ}{H}\right\} = \frac{1}{\triangle y}\left\{\lambda_{21}\frac{(PQ)_{i+1/2,j+1}^n}{H_{i+1/2,j+1}^n} + \lambda_{22}\frac{(PQ)_{i+1/2,j}^n}{H_{i+1/2,j}^n} + \lambda_{23}\frac{(PQ)_{i+1/2,j-1}^n}{H_{i+1/2,j-1}^n}\right\} \quad (2.24)$$

$$\frac{\partial}{\partial x}\left\{\frac{PQ}{H}\right\} = \frac{1}{\triangle x}\left\{\lambda_{31}\frac{(PQ)_{i+1,j+1/2}^n}{H_{i+1,j+1/2}^n} + \lambda_{32}\frac{(PQ)_{i,j+1/2}^n}{H_{i,j+1/2}^n} + \lambda_{33}\frac{(PQ)_{i-1,j+1/2}^n}{H_{i-1,j+1/2}^n}\right\} \quad (2.25)$$

9

$$\frac{\partial}{\partial y}\left\{\frac{Q^2}{H}\right\} = \frac{1}{\Delta y}\left\{\lambda_{41}\frac{(Q^n_{i,j+3/2})^2}{H^n_{i,j+3/2}} + \lambda_{42}\frac{(Q^n_{i,j+1/2})^2}{H^n_{i,j+1/2}} + \lambda_{43}\frac{(Q^n_{i,j-1/2})^2}{H^n_{i,j-1/2}}\right\} \tag{2.26}$$

in which the coefficient, λ, are determined from

$$\begin{cases} \lambda_{11} = 0, \lambda_{12} = 1, \lambda_{13} = -1, & if \quad P^n_{i+1/2,j} \geq 0 \\ \lambda_{11} = 1, \lambda_{12} = -1, \lambda_{13} = 0, & if \quad P^n_{i+1/2,j} < 0 \end{cases} \tag{2.27}$$

$$\begin{cases} \lambda_{21} = 0, \lambda_{22} = 1, \lambda_{23} = -1, & if \quad Q^n_{i+1/2,j} \geq 0 \\ \lambda_{21} = 1, \lambda_{22} = -1, \lambda_{23} = 0, & if \quad Q^n_{i+1/2,j} < 0 \end{cases} \tag{2.28}$$

$$\begin{cases} \lambda_{31} = 0, \lambda_{32} = 1, \lambda_{33} = -1, & if \quad P^n_{i,j+1/2} \geq 0 \\ \lambda_{31} = 1, \lambda_{32} = -1, \lambda_{33} = 0, & if \quad P^n_{i,j+1/2} < 0 \end{cases} \tag{2.29}$$

$$\begin{cases} \lambda_{41} = 0, \lambda_{42} = 1, \lambda_{43} = -1, & if \quad Q^n_{i,j+1/2} \geq 0 \\ \lambda_{41} = 1, \lambda_{42} = -1, \lambda_{43} = 0, & if \quad Q^n_{i,j+1/2} < 0 \end{cases} \tag{2.30}$$

Since the upwind scheme is employed, the discretized momentum equations are only first-order in accuracy in terms of spatial grid sizes. Bottom frictional terms are discretized as

$$F_x = \nu_x(P^{n+1}_{i+1/2,j} + P^n_{i+1/2,j}) \tag{2.31}$$

$$F_y = \nu_y(Q^{n+1}_{i,j+1/2} + Q^n_{i,j+1/2}) \tag{2.32}$$

where ν_x and ν_y are given by

$$\nu_x = \frac{1}{2}\frac{gn^2}{(H^n_{i+1/2,j})^{7/3}}[(P^n_{i+1/2,j})^2 + (Q^n_{i+1/2,j})^2]^{1/2} \tag{2.33}$$

$$\nu_y = \frac{1}{2}\frac{gn^2}{(H^n_{i,j+1/2})^{7/3}}[(P^n_{i,j+1/2})^2 + (Q^n_{i,j+1/2})^2]^{1/2} \tag{2.34}$$

for the Manning's formula. Finally, the finite difference forms for the continuity and momentum equations in Cartesian Coordinates are written as

$$\eta^{n+1/2}_{i,j} = \eta^{n-1/2}_{i,j} - r_x(P^n_{i+1/2,j} - P^n_{i-1/2,j}) - r_y(Q^n_{i,j+1/2} - Q^n_{i,j-1/2}) \tag{2.35}$$

10

$$P_{i+1/2,j}^{n+1} = \frac{1}{1 + \nu_x \Delta t} \left\{ (1 - \nu_x \Delta t) P_{i+1/2,j}^n - r_x g H_{i+1/2,j}^{n+1/2} (\eta_{i+1,j}^{n+1/2} - \eta_{i,j}^{n+1/2}) \right\}$$

$$- \frac{r_x}{1 + \nu_x \Delta t} \left\{ \lambda_{11} \frac{(P_{i+3/2,j}^n)^2}{H_{i+3/2,j}^n} + \lambda_{12} \frac{(P_{i+1/2,j}^n)^2}{H_{i+1/2,j}^n} + \lambda_{13} \frac{(P_{i-1/2,j}^n)^2}{H_{i-1/2,j}^n} \right\}$$

$$- \frac{r_x}{1 + \nu_x \Delta t} \left\{ \lambda_{21} \frac{(PQ)_{i+1/2,j+1}^n}{H_{i+1/2,j+1}^n} + \lambda_{22} \frac{(PQ)_{i+1/2,j}^n}{H_{i+1/2,j}^n} + \lambda_{23} \frac{(PQ)_{i+1/2,j-1}^n}{H_{i+1/2,j-1}^n} \right\} \qquad (2.36)$$

$$Q_{i,j+1/2}^{n+1} = \frac{1}{1 + \nu_y \Delta t} \left\{ (1 - \nu_y \Delta t) Q_{i,j+1/2}^n - r_y g H_{i,j+1/2}^{n+1/2} (\eta_{i,j+1}^{n+1/2} - \eta_{i,j}^{n+1/2}) \right\}$$

$$- \frac{r_y}{1 + \nu_y \Delta t} \left\{ \lambda_{31} \frac{(PQ)_{i+1,j+1/2}^n}{H_{i+1,j+1/2}^n} + \lambda_{32} \frac{(PQ)_{i,j+1/2}^n}{H_{i,j+1/2}^n} + \lambda_{33} \frac{(PQ)_{i-1,j+1/2}^n}{H_{i-1,j+1/2}^n} \right\}$$

$$- \frac{r_y}{1 + \nu_y \Delta t} \left\{ \lambda_{41} \frac{(Q_{i,j+3/2}^n)^2}{H_{i,j+3/2}^n} + \lambda_{42} \frac{(Q_{i,j+1/2}^n)^2}{H_{i,j+1/2}^n} + \lambda_{43} \frac{(Q_{i,j-1/2}^n)^2}{H_{i,j-1/2}^n} \right\} \qquad (2.37)$$

in which $r_x = \Delta t / \Delta x$ and $r_y = \Delta t / \Delta y$. Following approximations have been used to derive the above finite difference equations.

$$H_{i+1/2,j}^{n+1/2} = \frac{1}{2}(H_{i,j}^{n+1/2} + H_{i+1,j}^{n+1/2}) \qquad (2.38)$$

$$H_{i,j+1/2}^{n+1/2} = \frac{1}{2}(H_{i,j}^{n+1/2} + H_{i,j+1}^{n+1/2}) \qquad (2.39)$$

$$H_{i+1/2,j}^{n} = \frac{1}{4}(H_{i,j}^{n-1/2} + H_{i,j}^{n+1/2} + H_{i+1,j}^{n-1/2} + H_{i+1,j}^{n+1/2}) \qquad (2.40)$$

$$H_{i,j+1/2}^{n} = \frac{1}{4}(H_{i,j}^{n-1/2} + H_{i,j}^{n+1/2} + H_{i,j+1}^{n-1/2} + H_{i,j+1}^{n+1/2}) \qquad (2.41)$$

$$P_{i,j+1/2}^{n} = \frac{1}{4}(P_{i-1/2,j}^{n} + H_{i-1/2,j+1}^{n} + P_{i+1/2,j}^{n} + P_{i+1/2,j+1}^{n}) \qquad (2.42)$$

$$Q_{i+1/2,j}^{n} = \frac{1}{4}(Q_{i,j-1/2}^{n} + Q_{i+1,j-1/2}^{n} + Q_{i,j+1/2}^{n} + Q_{i+1,j+1/2}^{n}) \qquad (2.43)$$

In spherical coordinates, the nonlinear shallow water equations are discretized as

$$\eta_{i,j}^{n+1/2} = \eta_{i,j}^{n-1/2} - \frac{1}{R \cos \varphi_{i,j}} \frac{\Delta t}{\Delta \psi}(P_{i+1/2,j}^{n} - P_{i-1/2,j}^{n})$$

$$- \frac{1}{R} \frac{\Delta t}{\Delta \varphi}(Q_{i,j+1/2}^{n} - Q_{i,j-1/2}^{n}) \qquad (2.44)$$

$$P_{i+1/2,j}^{n+1} = f_x \left\{ (1 - \nu_x \Delta t) P_{i+1/2,j}^{n} - \left\{ \frac{gH}{R \cos \varphi} \right\}_{i+1/2,j}^{n+1/2} \frac{\Delta t}{\Delta \psi}(\eta_{i+1,j}^{n+1/2} - \eta_{i,j}^{n+1/2}) \right\}$$

$$- \frac{f_x}{R \cos \varphi_{i,j}} \frac{\Delta t}{\Delta \psi} \left\{ \lambda_{11} \frac{(P_{i+3/2,j}^n)^2}{H_{i+3/2,j}^n} + \lambda_{12} \frac{(P_{i+1/2,j}^n)^2}{H_{i+1/2,j}^n} + \lambda_{13} \frac{(P_{i-1/2,j}^n)^2}{H_{i-1/2,j}^n} \right\}$$

11

$$-\frac{f_x}{R}\frac{\triangle t}{\triangle \varphi}\left\{\lambda_{21}\frac{(PQ)^n_{i+1/2,j+1}}{H^n_{i+1/2,j+1}}+\lambda_{22}\frac{(PQ)^n_{i+1/2,j}}{H^n_{i+1/2,j}}+\lambda_{23}\frac{(PQ)^n_{i+1/2,j-1}}{H^n_{i+1/2,j-1}}\right\} \quad (2.45)$$

$$Q^{n+1}_{i,j+1/2}=f_y\left\{(1-\nu_y\triangle t)Q^n_{i,j+1/2}-\frac{gH^{n+1/2}_{i,j+1/2}}{R}\frac{\triangle t}{\triangle \psi}(\eta^{n+1/2}_{i,j+1}-\eta^{n+1/2}_{i,j})\right\}$$

$$-\frac{f_y}{R\cos\varphi_{i,j+1/2}}\frac{\triangle t}{\triangle \psi}\left\{\lambda_{31}\frac{(PQ)^n_{i+1,j+1/2}}{H^n_{i+1,j+1/2}}+\lambda_{32}\frac{(PQ)^n_{i,j+1/2}}{H^n_{i,j+1/2}}+\lambda_{33}\frac{(PQ)^n_{i-1,j+1/2}}{H^n_{i-1,j+1/2}}\right\}$$

$$-\frac{f_y}{R}\frac{\triangle t}{\triangle \varphi}\left\{\lambda_{41}\frac{(Q^n_{i,j+3/2})^2}{H^n_{i,j+3/2}}+\lambda_{42}\frac{(Q^n_{i,j+1/2})^2}{H^n_{i,j+1/2}}+\lambda_{43}\frac{(Q^n_{i,j-1/2})^2}{H^n_{i,j-1/2}}\right\} \quad (2.46)$$

in which $f_x=\frac{1}{1+\nu_x\triangle t}$ and $f_y=\frac{1}{1+\nu_y\triangle t}$. Other variables are the same as defined before.

2.3   Nested Grid Configuration

As we know during the shoaling of waves, their length will become much smaller than in deep ocean. Finer grids will be necessary to resolve wave profiles in shallow water regions. Therefore, when the water depth varies within the computational domain, it might be desirable that different grid size and time step size be employed in different sub-regions. The nested grid configuration allows to obtain detailed information in the coastal region. Finer grids should be used only in specific regions of interests.

In COMCOT, either the linear or nonlinear shallow water equations with either spherical or cartesian coordinate system can be assigned to a specific sub-level region. These sub-level grid regions are dynamically connected. The any ratio of grid size between two directly nested grid layers can be used, however it should be an integer.

Here we briefly describe the technique for exchanging information between two nested grid layers of different grid sizes. As shown in Figure 2.2 and 2.3, a smaller grid system is nested in a larger grid system with the ratio of 1 : 3. The arrows represent the volume fluxes, P and Q, across each grid cell, while squares and dots indicate the
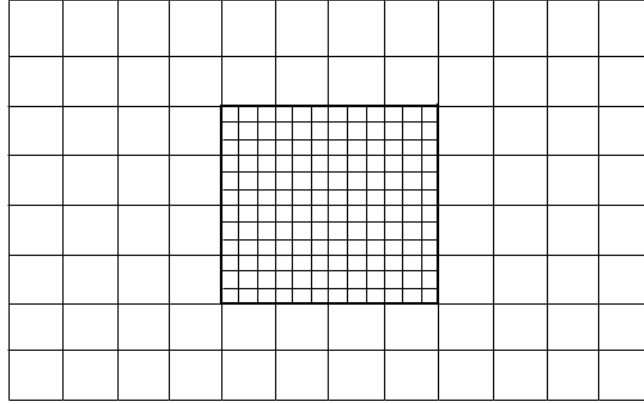
Figure 2.2: Sketch of Nested Grid Setup

—— Connecting boundary	■ Center of parent grid	⇑ Volume Flux of Parent Grid	↑ Volume Flux of Sub-level Grid
	• Center of sub-level grid		
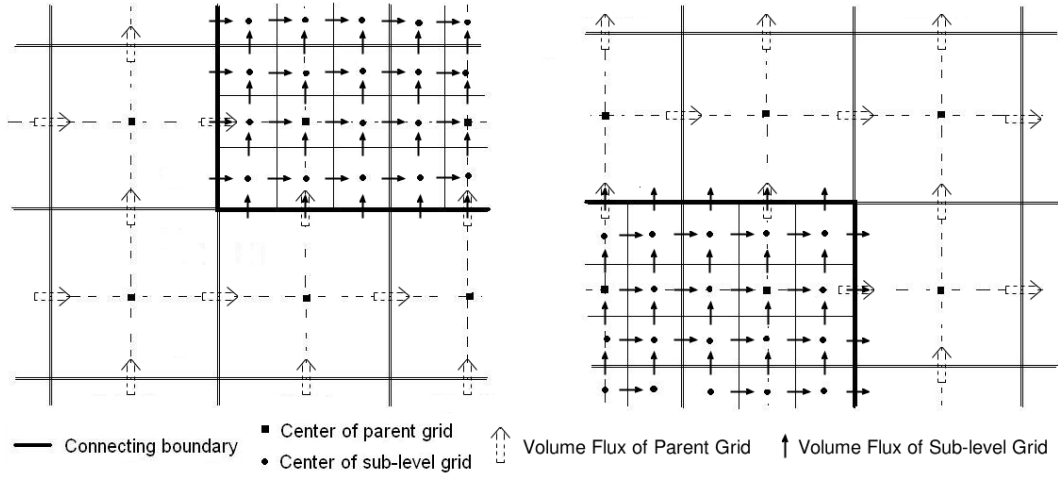
Figure 2.3: Detailed view of Nested Grid Setup. Left panel: grid nesting at lower-left corner of sub-level grid region; Right panel: grid nesting at upper-right corner of sub-level grid region.

locations where the free surface displacement is evaluated.

At a certain time level, volume fluxes in both large and small grid systems are determined from the momentum equations, with the exception of volume fluxes for the smaller grid system along the boundaries between two grid regions. These data are de-

termined by interpolating the neighboring volume fluxes from the large grid system. The free surface displacement at the next time level for the small grid system can be calculated from the continuity equation. Usually the time step size for the smaller grid system is also smaller than that used in the larger grid system to sastify the CFL (Courant-Friedrichs-Lewy) condition. Therefore, the volume fluxes along the boundary of the small grid system at the next time level must be obtained by interpolating the neighboring volume fluxes obtained from the large grid system over a larger time interval. After the free surface displacements in the small grid system are calculated up tot he next time level of the large grid system, the free surface displacements in the large grid system are updated by solving the continuity equation.

Let us describe these procedure step by step. Suppose all flux values in the inner and the outer region are known at time level $t = n\triangle t$ and we need to solve the inner and the outer region values at the next time step $t = (n + 1)\triangle t$. Since the outer grid region and the inner grid region adopt different grid sizes, the time step sizes for each region are different due to the requirement of stability. In COMCOT, the ratio of time step size between the outer grid region and inner grid region varies, depending on the maximum water depth in each region. And for simplicity, also assume that the time step of the inner region is one half of that of the outer region (see Figure 2.4).

*Get the free surface elevation at $t = (n + 1/2)\triangle t$ in the outer region by solving continuity equation.

*To solve the continuity equation in the inner region, however, we need to have the flux information along the connected boundary at $t = n\triangle t$. So the flux values in the outer grids at the connected boundary are linearly interpolated and then those interpolated values are assigned to the fluxes in the inner at the boundary.

*Get the free surface elevation at $t = (n + 1/4)\triangle t$ in the inner grid region by solving continuity equation.

*Get the flux values at $t = (n+1/2)\triangle t$ in the inner grid region by solving momentum equation.

*To get the free surface elevation at $t = (n + 3/4)\triangle t$ in the inner grid region, we should have the flux information along the connected boundary at $t = (n + 1/2)\triangle t$. To get these information we can do the in the following way. First, since we already know the free surface elevation at $t = (n+1/2)\triangle t$ and flux at $t = n\triangle t$ in the outer region, we can get the flux in the outer region along the connected boundary at $t = (n + 1\triangle t)$ by solving linear momentum equation locally. Second, these flux values at $t = (n+1)\triangle t$ are linearly interpolated along the connected boundary. And to get the value at $t = (n+1/2)\triangle t$, outer flux values at $t = n\triangle t$ and $t = (n+1)\triangle t$ are also linearly interpolated. Those spatially and timely interpolated flux values are assigned to the flux in the inner grid at the boundary.

*Get the free surface elevation at $t = (n + 3/4)\triangle t$ in the inner grid region by solving continuity equation.

*To transfer the information from the inner grid region to the outer region, the free surface elevation in the inner grid region is spatially averaged over the grid size of the outer region. These averaged elevation values at $t = (n + 3/4)\triangle t$ are then time averaged with those at $t = (n + 1/4)\triangle t$ in the inner region. These spatially and timely averaged elevation values in the inner grid region update the elevation values at $t = (n + 1/2)\triangle t$ in the outer region.

*Get the flux values at $t = (n + 1)\triangle t$ in the inner region by solving momentum equation;

*Get the flux values at $t = (n + 1)\triangle t$ in the outer region by solving momentum equation.

The above scheme of time and space evoluation for nested grids is illustrated in Figure 2.4 for 1-D problem. This nested grid scheme has been validated and applied to
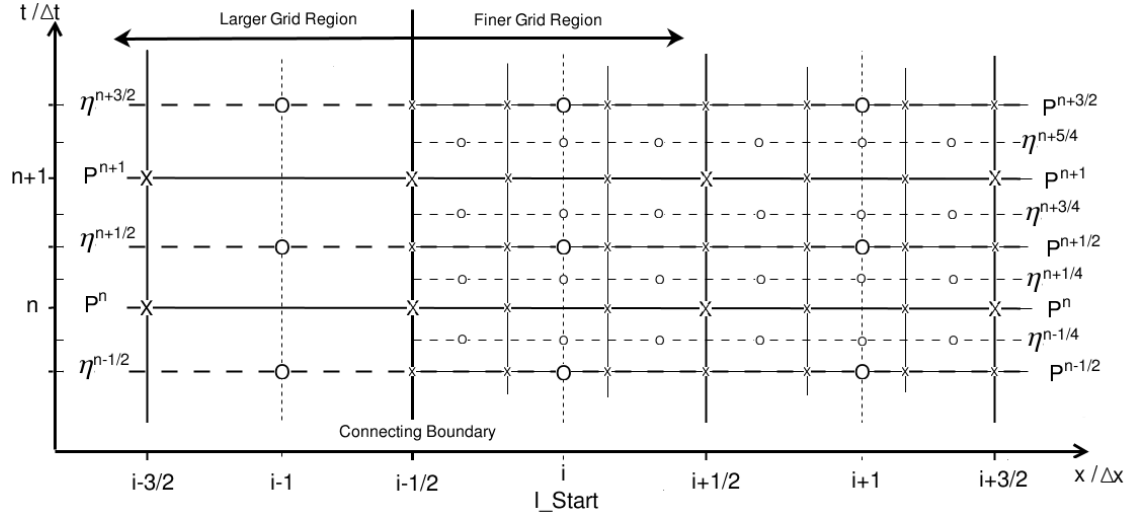
Figure 2.4: Detailed Time Marching Scheme of Nested Grid Setup.

several numerical, experimental and practical studies (Liu et al., 1994, 1995; Cho, 1995; Liu et al., 1998; Wang and Liu, 2005, 2007).

2.4 Moving Boundary Scheme

In carrying out numerical computations, the computational domain is divided into finite difference grids. Initially, the free surface displacement is zero everywhere, as are the volume fluxes. When the grid point is on dry land, the 'water depth', h, takes a negative value and gives the elevation of the land measured from the Mean Water Level (MWL). Figure 2.5 shows a schematic sketch of the moving boundary treatment used in the

16

study (Cho, 1995; Liu et al., 1995). The MWL represents the mean water level and H_f denotes the flooding depth in Figure 2.5. In a land (dry) cell the total depth, $H = h + \eta$, has a negative value. On the other hand, the wet cell has a positive H value. The continuity equation in conjunction with boundary conditions along offshore boundaries is used to find free surface displacements at the next time step in the entire computational domain, including the dry (land) cells. The free surface displacement at a dry land grid remains zero because the volume fluxes are zero at the neighboring grid points (See figure 2.5). At a shoreline grid, the total depth, H, is updated. A numerical algorithm is needed to determine if the total water depth is high enough to flood the neighboring dry (land) cells and hence to move the shoreline. The momentum equations are used to update the volume fluxes in the wet cells only.

To illustrate the moving boundary algorithm, the one-dimensional case is used as an example. As shown in Figure 2.5, the real bathymetry has been replaced by a staircase representation. The total depth, H, is calculated and recorded at grid points $i - 1$, i and $i + 1$, while the volume flux is computed at grid points $i - 1/2$, $i + 1/2$ and $i + 3/2$. As shown in Figure 2.5), the $i - th$ cell is a wet cell in which the total depth is positive and the $(i + 1) - th$ cell is dry (land) cell in which the total depth is negative and the volume fluxes are zero. The shoreline is somewhere between the $i - th$ cell and $(i + 1) - th$ grid points. Then, the volume flux at the $(i - 1/2) - th$ grid point is assigned to be zero. Therefore, the shoreline does not move to the onshore direction. When the water surface is rising as shown in Figure 2.5, however, the volume flux at the $(i + 1/2) - th$ grid point is no longer zero. The shoreline may move one grid point to the onshore direction. After the total depth has been updated from the continuity equation, the following algorithm is used to determine whether or not the shoreline should be moved. If $H_i > 0$, possible cases can be summarized as
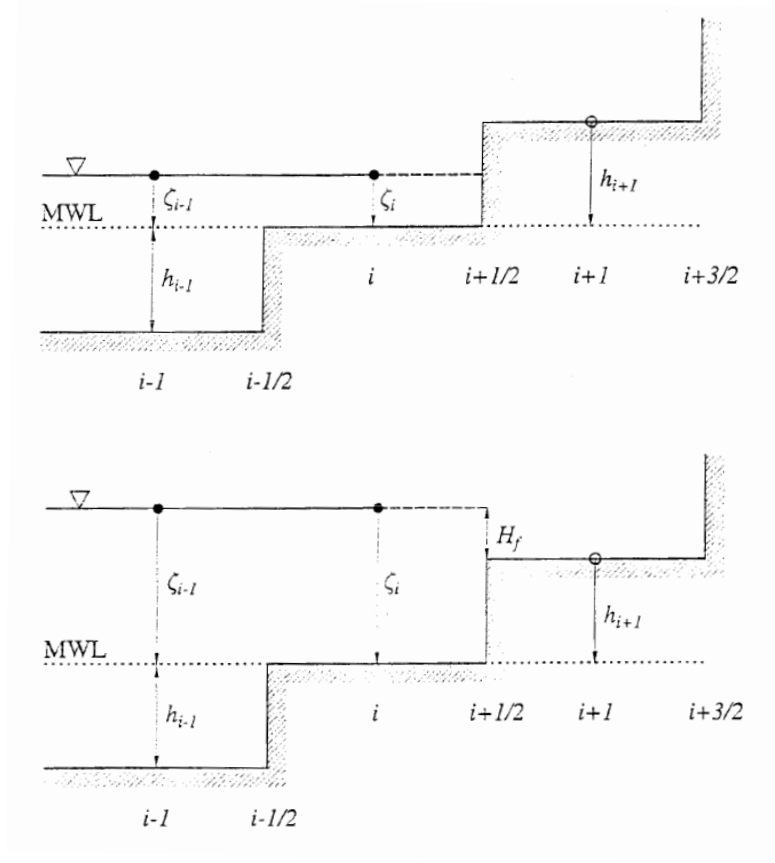
Figure 2.5: A sketch of moving boundary scheme.

* If $H_{i+1} \leq 0$ and $h_{i+1} + \eta_i \leq 0$, then the shoreline remains between grid points i and $i + 1$ and the volume flux $P_{i+1/2}$ remains zero;

* If $H_{i+1} \leq 0$ and $h_{i+1} + \eta_i > 0$, then the shoreline moves to between grid points $i + 1$ and $i + 2$ and the volume flux $P_{i+1/2}$ may have a nonzero value, while $P_{i+3/2}$ is assigned to be zero. The flooding depth is $H_f = h_{i+1} + \eta_i$;

* If $H_{i+1} > 0$, then the shoreline moves to between grid points $i + 1$ and $i + 2$. The volume flux $P_{i+1/2}$ may have a nonzero value while $P_{i+3/2}$ has a zero value. The flooding depth is $H_f = max(h_{i+1} + \eta_i, h_{i+1} + \eta_{i+1})$.

In the above cases, the time-step index has been omitted for simplicity. The algo-

18

rithm is developed for a two-dimensional problem and the corresponding *y* direction algorithm has the same procedure as that for the *x* direction.

To save computing time, the regions that represent permanent dry (land) can be excluded from the computation by installing a depth criterion. In COMCOT, grid cells with land elevation greater than 50.0 meters, will not be included in the computation. Moreover, when *H* is very small, the associated bottom friction term become very large and, accordingly, a lower bound of the water depth is used to avoid the difficulty. The finite difference approximation for the continuity equation correctly accounts for positive and zero values of the total depth on each side of a computational grid. The treatment of flooding and ebbing grid cells guarantees mass conservation while accounting for the flooding and ebbing of land. The occurrence of a zero value for the total depth *H* on one side of a cell implies zero mass flux until *H* becomes positive. A grid cell is considered a dry cell only if the total water depths at all sides are zero or negative. This moving boundary scheme has been validated and applied to several experimental and practical studies (Liu et al., 1994, 1995; Cho, 1995; Wang and Liu, 2007).

2.5 Dispersion Improvement

For most tsunami events, length scales of tsunamis are much larger than water depth over which they propagate. Therefore, physical frequency dispersion effect can be neglected and Shallow Water Equations are adequate enough to describe tsunami waves without considering dispersion. However, the wavelength of a tsunami may not be large enough compared to water depth so that the dispersion effect can be neglected. Moveover, the dispersion effect is also accumulated over distance. Thus, in some conditions, the dispersion effect should be considered in a simulation. Physically, Boussinesq Equation

models or 3-D Navier-Stokes equation models are required to account for the dispersion effects. But considering the scale of a tsunami simulation and computational cost of these models, Boussinesq Equation models or 3-D Navier-Stokes equation models are not a preferable choice. As we know, numerical dispersion is an inherent phenomena in discretizing shallow water equation with explicit leap-frog finite difference scheme. Imamura et al. (1988) proposed a method to mimic physical dispersion by using this type of numerical dispersion for linear shallow water equation models over constant water depth. By choosing grid size according to the following relationship,

$$\triangle x = \sqrt{4h^2 + gh(\triangle t)^2} \tag{2.47}$$

in which h is water depth; g is gravitational acceleration and $\triangle t$ is the size of time step, then physical dispersion can be recovered. Cho (1995) improved the method to correct the accuracy in diagonal directions. Yoon (2002) further improve the scheme to describe the dispersion effect over a slowly varying bathymetry. Later on, Wang (2008) extended the idea to weakly nonlinear weakly dispersive waves over a slowly varying bathymetry so that the numerical dispersion in the shallow water equation model can be used to recover the dispersion relationship of traditional Boussinesq equations.

Please refer to Wang (2008) for more details.

CHAPTER 3

TSUNAMI GENERATION

Tsunamis are generated by large-area disturbances on seafloor, such as submarine earthquakes, landslides or volcanic eruptions, or on water surface such as meteorite impacts. Multiple tsunami generation mechanisms can be implemented in COMCOT, including instantaneous seafloor rupture computed via fault models, e.g., Okada (1985) and Mansinha and Smylie (1971), transient floor motions (e.g., transient ruptures, landslides), customized profiles of water surface displacements and wave makers.

3.1 Sea Floor Disturbances

Depending on the duration of the seafloor motion relative to the wave period of tsunamis, the seafloor disturbances can be classified into two categories. If the duration of a floor motion is much shorter the tsunami wave period being generated, the motion can be assumed instantaneous (i.e., a sudden uplift of seafloor), then the displacement of seafloor can be estimated via fault models (Mansinha and Smylie, 1971; Okada, 1985) and the water surface is assumed to exactly follow the uplift the seafloor since water over this large rupture area can not be drained out within such short duration. However, if the duration of the floor rupture motion is comparable to tsunami wave period, the rupture should be considered as a transient process and this transient process should be modelled in tsunami simulations.

3.1.1   Instantaneous Deformation - Elastic Fault Model

For instantaneous seafloor rupture, the seafloor displacement caused by an earthquake event is computed via elastic finite fault plane theory proposed originally by Mansinha and Smylie (1971) and then improved by Okada (1985). Both models are available in COMCOT. The theory assumes a rectangular fault plane being buried in semi-infinite elastic half plane. This plane is an idealized representation of the interface between two colliding tectonic plates where violent relative motion (i.e., dislocation) occurs during an earthquake event (see Figure 3.1). The dislocation (or slip motion) occurring on the fault plane will then deform the surface of the semi-infinite medium, which is considered as the seafloor displacement during the earthquake event. To compute the deformation, the following fault parameters are necessary. The definition of these parameters can be seen

Table 3.1: Parameters for Elastic Fault Plane Model

Parameters	Unit
Epicenter (Lat, Lon)	Degrees
Focal depth	Meters
Length of Fault Plane	Meters
Width of Fault Plane	Meters
Dislocation (slip)	Meters
Strike direction (θ)	Degrees
Dip angle (δ)	Degrees
Rake (slip) angle (λ)	Degrees

in Figure 3.1. In elastic fault plane theory, *fault plane* is where violent relative motion occurs in an earthquake event. Specifically, fault plane is assumed as an rectangular area of plate interface on foot block and the top and bottom edges of the fault plane are parallel to the mean Earth surface. The orientation and position of this fault plane are

prescribed by its center location (φ_0, ψ_0), strike direction and dip angle. The center of the fault plane is called *focus* and is the location where rupture starts during an earthquake event. Its projection on the mean surface of the Earth is called *epicenter*. *Focal depth* is defined as the vertical distance between the focus and the epicenter. *Strike direction* is defined as the facing direction when someone stands on the top edge of a fault plane with foot block on his left-hand side and the fault plane on his right-hand side. Then *strike angle*, θ, is the angle measuring clockwise from the local north to the strike direction. *Dip angle*, δ, is the angle between the mean Earth surface and the fault plane, measured from the mean Earth surface down to the fault plane. The size of the fault plane is described by its length and width. The *length* of a fault plane, L, is defined as the length of its top edge or bottom edge (the edges parallel to the strike direction) and the *width* of the fault plane, W, refers to the length of one of the other two edges. The above parameters describe the size, location and orientation of a fault plane. The rupture occurring on this fault plane is described by slip direction (i.e., rake) and dislocation (amount of slip motion). *Slip Direction (rake)* describes to which direction the hanging block moves relative to the foot block on the fault plane. *Strike angle*, λ, is the angle measured counter-clock-wise from strike direction to slip direction on the fault plane. *Dislocation (slip amount)* is the distance of motion of hanging block relative to the foot block along the strike direction on the fault plane.

With the fault parameters defined above, the seafloor deformation can be calculated via elastic finite fault plane theory. The detailed procedure of this calculation can be found in the papers by Mansinha and Smylie (1971) and Okada (1985).

Since the floor displacement is evaluated over a plane, special handling is required to map it onto the mean Earth Surface (i.e., Ellipsoidal surface). Oblique Stereographic Projection (Snyder, 1987) is implemented in COMCOT to map the surface of

an Ellipsoid (the Earthquake) onto a plane by taking the epicenter as where the plane is tangential to the Earth surface. For this projection in COMCOT, the Earth is described by WGS84 Datum (i.e., semi-major axis $a = 6378137.0m$ and semi-minor axis $b = 6356752.3142m$ with scaling factor $k_0 = 0.9996$). With this projection method, each location (φ, λ) on the Earth surface (Ellipsoidal surface), corresponds to a point (x, y) on the plane tangential to the Earth surface at the epicenter (φ_0, λ_0), whose displacement can be computed via either Mansinha and Smylie's method or Okada's approach.

3.1.2   Transient Seafloor Motion

Different from the instant deformation in which the duration of rupturing process can be neglected, for a transient seafloor motion, the duration cannot be omitted and should be considered in numerical simulations. This type of transient seafloor motion could be the seafloor rupture caused by an earthquake event or submarine landslides. The inclusion of temporal variation of water depth (or, more exactly, the motion of seafloor) in Equations (2.1)-(2.13) allows to simulate such type of transient bottom floor motion as long as long wave assumption is satisfied. This transient seafloor motion model has been applied to study the transient rupture process of the 2004 Indian Ocean tsunami (Wang and Liu, 2006).

To simulate tsunamis generated by transient seafloor motion with COMCOT, variation of water depth in terms of time should be prepared before a simulation starts. The input data file contains a sequence of snapshots of instantaneous seafloor positions relative to its original position. This snapshot data is then used to evaluate the term $\frac{\partial h}{\partial t}$ in Equations (2.1)-(2.13). Figure 3.2 shows how water depth changes during a landslide event. Three snapshots are presented in the sketch. The variations of seafloor in this event are

described by its position relative to its original location. For example, in snapshot $t = t2$, the seafloor variations at $x = x1, x2, x3$ are given as $\triangle h(x1, t2) = h(x1, t0) - h(x1, t2)$, $\triangle h(x2, t2) = h(x2, t0) - h(x2, t2)$ and $\triangle h(x3, t2) = h(x3, t0) - h(x3, t2)$, respectively. If $\triangle h > 0$, it means seafloor is being uplifted; if $\triangle h < 0$, the seafloor is being subsided.

3.2   Water Surface Disturbances

In addition to generating tsunamis via seafloor motions, in COMCOT, tsunamis can also be generated from a customized initial water surface displacement. When using this mechanism to generate a tsunami, a data file needs to be prepared which contains the the profile of water surface displacement measured from the mean surface level. This displacement will become the source of a tsunami.

LEGEND
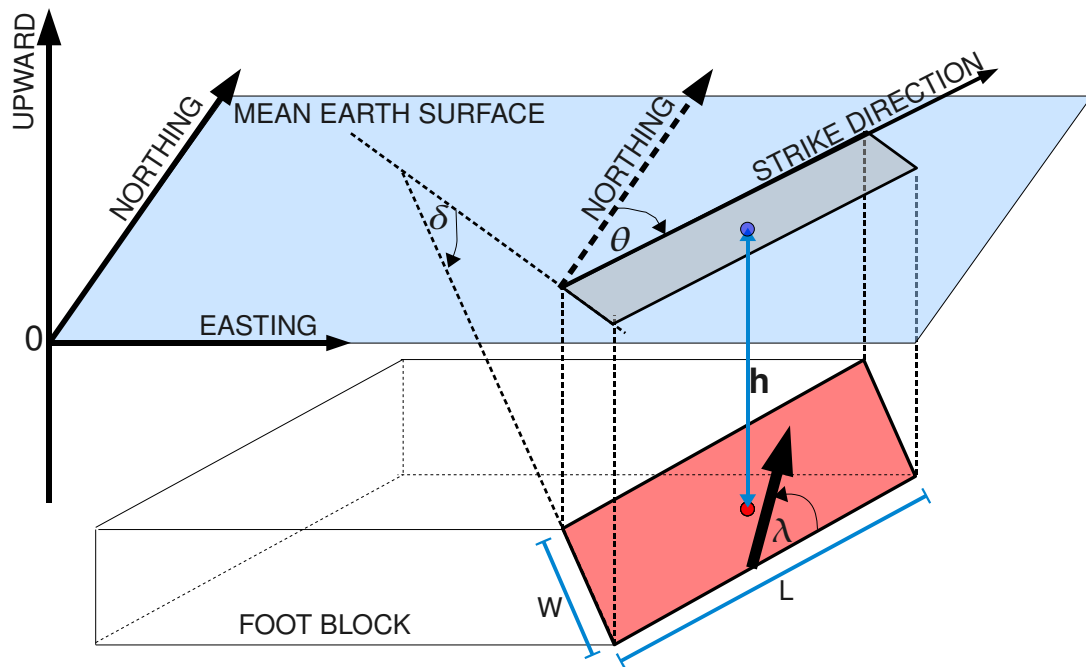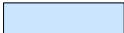
(light blue box)	MEAN EARTH SURFACE
(red box)	FAULT PLANE (A RECTANGULAR SURFACE ON FOOT BLOCK)
(gray box)	PROJECTION OF FAULT PLANE ON MEAN EARTH SURFACE
(black arrow)	SLIP DIRECTION ON FAULT PLANE (RELATIVE TO FOOT BLOCK)
(red dot)	FOCUS OF AN EARTHQUAKE (CENTER OF FAULT PLANE)
(blue dot)	EPICENTER (PROJECTION OF FOCUS ON EARTH SURFACE)
δ	DIP ANGLE OF FAULT PLANE
λ	SLIP DIRECTION ON FAULT PLANE (RAKE ANGLE)
θ	STRIKE ANGLE
h	FOCAL DEPTH
L	LENGTH OF FAULT PLANE
W	WIDTH OF FAULT PLANE

Figure 3.1: Sketch of a Fault Plane and Fault parameter definitions.

26
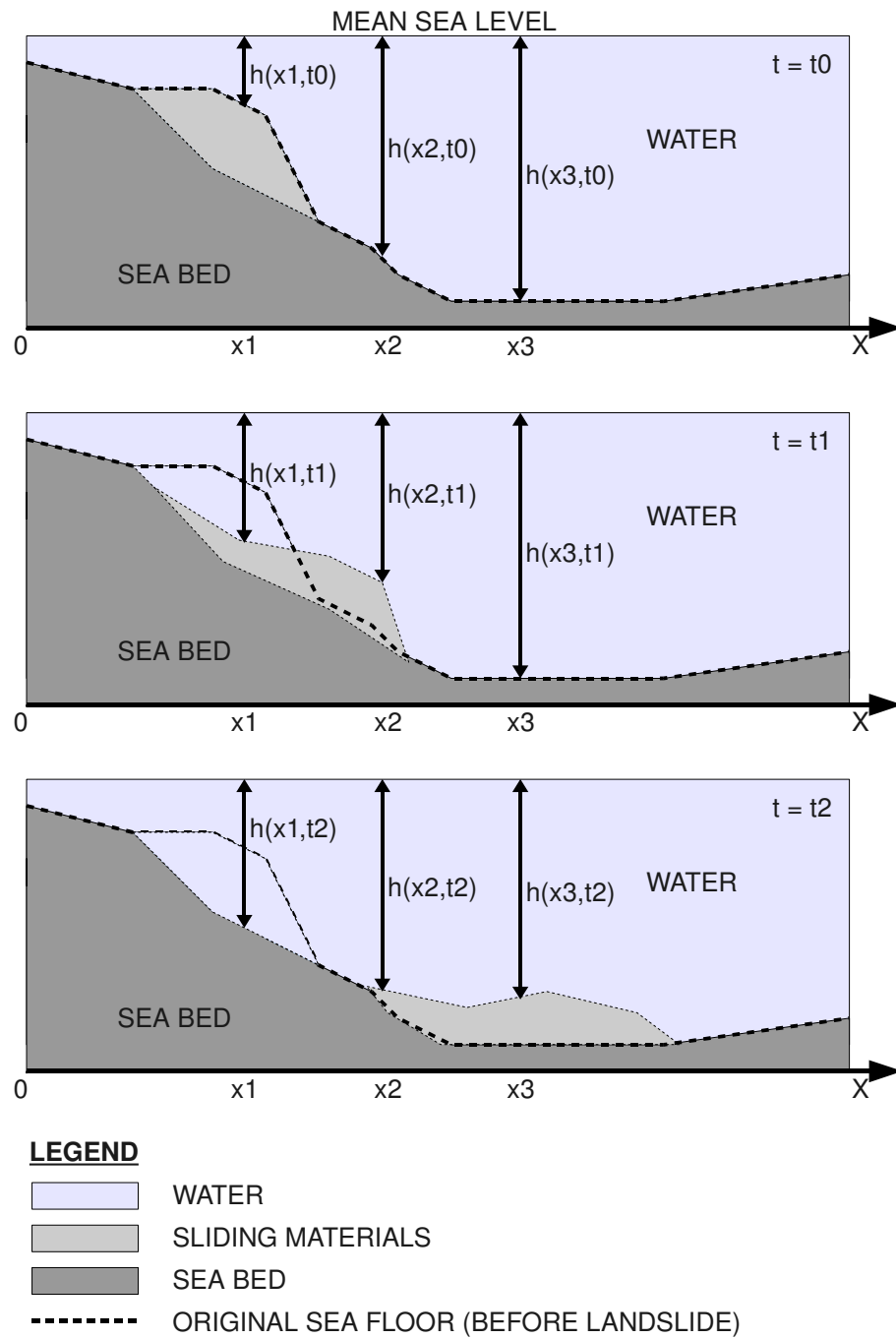
Figure 3.2: Sketch of Transient Sea Floor Motion).

CHAPTER 4

PARAMETER CONFIGURATION, INPUT AND OUTPUT DATA

The user should prepare the topographic information and focal parameters for the specific tsunami simulation. The detailed information on preparing these files, as well as a further explanation of the items in input files is given in the follows sections.

4.1 Control Files

COMCOT.CTL defines all the parameters required for tsunami simulations with COMCOT. If multiple fault planes are implemented, an additional control file, ***FAULT_MULTI.CTL***, is also required to configure parameters for additional fault planes. These two parameter control files can be edited or viewed with any TXT-editing applications, such as ***WordPad***, ***UltraEdit*** and etc. It should be noted the structure of these two files CANNOT be altered or changed except for the ***VALUE FIELD*** portion. Otherwise, COMCOT cannot read these two files properly.

In general, ***COMCOT.CTL*** contains 5 parameter sections, which provides control on the parameters for the simulation, fault model, wave maker, landslides and grid setup. Each section will be explained in detail in the following sections.

4.1.1 General Information

The first section (see Figure 4.1) in ***COMCOT.CTL*** provides the control on the general aspects of a numerical simulation, such as the total runtime, initial and boundary conditions. For each line, parameter value should be specified after ':'.

```
##################################################
#                                                #
# Control file for COMCOT program (v1.7)         #
#                                                #
##################################################
#--+-----1----+----2----+----3----+----4----+----5----+----6----+-
#===================================================:=================
# General Parameters for Simulation                 : Value Field
#===================================================:=================
#Job Description: NZ30sec bathymetry... for code testing
 Total run time (Wall clock, seconds)              :   7200.000
 Time interval to Write Data    ( unit: sec )      :     60.0
 Output Zmax & TS(0-Max. Z;1-Timeseries;2-Both ):      0
 Start Type (0-Cold start; 1-Hot start)            :      0
 Resuming Time If hot start (Seconds)              :   3000.00
 Specify Min WaterDepth offshore  (meter)          :     10.00
 Initial Cond. (0:FLT,1:File,2:WM,3:LS,4:FLT+LS):      0
 Specify BC  (0-Open;1-Sponge;2-Wall;3-FACTS)   :      0
 Specify Input Z filename (for BC=3, FACTS)     : 23926h.asc
 Specify Input U filename (for BC=3, FACTS)     : 23926u.asc
 Specify Input V filename (for BC=3, FACTS)     : 23926v.asc

#===================================================:=================
```

Figure 4.1: General Parameter Section in *COMCOT.CTL*

Total run time defines the total physical duration to be simulated, which should be given in seconds.

Time interval to Write Data defines the time interval (in seconds) to output data (including water surface elevation, and volume flux if specified).

Output Zmax & TS is used to control the output of maximum water surface elevation and time history records at given locations. 0 – The maximum water surface elevation and depression will be output every hour; 1 – The the time history records will be output at up to 9999 locations given in the data file *ts_location.dat*; 2 – Both the maximum water surface elevation and the time history records will be output.

Start Type is used to specify the starting type of a simulation. 0 – Start a simulation from the very beginning, $t = 0s$; 1 – Start a simulation from a resuming time step where data are previously saved.

Resuming Time If hot start specified the moment when a simulation starts from if

hot start is used or, the moment when a snapshot will be saved for a later restart if cold start is selected.

Specify Min WaterDepth offshore is used to define the where is the shoreline. For example, if a value 10.0 is assigned here, the water depth shallower than 10.0 meters will be treated as land region and a vertical wall boundary is set along the $10.0 - meter$ water depth contour. To specify the true shoreline, 0.0 should be given here which will be used for runup and inundation calculation.

Initial Cond. (0:FLT,1:File,2:WM,3:LS,4:FLT+LS) is used to define the initial conditions. 0 – use fault model to calculate the seafloor deformation and fault parameters should be given at fault parameter section in COMCOT.CTL; If multiple fault planes are implemented, parameters for additional fault planes should be given in FAULT_MULTI.CTL; 1 – use customized the profile in an external data file as initial condition and the file name and format are specified at Fault Parameter section; 2 – use incident wave maker to generate waves; 3 – use landslide model to generate tsunamis and landslide parameters are defined at Landslide section in COMCOT.CTL; 4 – use both fault model and landslide model to generate tsunamis.

Specify BC (0-Open;1-Sponge;2-Wall;3-FACTS) is used to define boundary conditions of the numerical domain. 0 – open boundary (i.e., radiation boundary); 1 – use sponge layer (absorbing boundary); 2 – use vertical wall boundary; 3 – use FACTS data as input boundary condition for far-field tsunami sources and use COM-COT to calculate nearshore properties. The input boundary conditions are obtained from the data files given at **Specify Input Z filename**, **Specify Input U filename** and **Specify Input V filename**.

4.1.2   Parameters for Fault Model

If in the line **Initial Cond. (0:FLT,1:File,2:WM,3:LS,4:FLT+LS)** in General Parameter Section, 0 or 4 is selected, fault parameters should be given in the section **Parameters for Fault Model** in COMCOT.CTL. These fault parameters will be used to calculate seafloor deformation during an earthquake event. Then, it is assumed that the water surface just mimics the seafloor deformation.

```
#=========================================:============================
# Parameters for Fault Model (Segment 01)        :Values                                    |
#=========================================:============================
No. of FLT Planes (With fault_multi.ctl if >1) :    1
Fault Rupture Time (seconds)                   :    0.0
Faulting Option (0: Model; 1- Data;)           :    0
Focal Depth                          (meter):   15000.000
Length of source area                (meter):   40000.000
Width of source area                 (meter):   20000.000
Dislocation of fault plate           (meter):       5.300
Strike direction (theta)            (degree):     210.100
Dip  angle       (delta)            (degree):      40.000
Slip angle       (lamda)            (degree):      90.000
Comp. Domain- Left Edge - Latitude  (degree):     -40.5
Comp. Domain- South Edge - Longitude (degree):    176.0
Epicenter Location: Latitude        (degree):     -39.40
Epicenter Location: Longitude       (degree):     177.95
File Name of Deformation Data       : wholemargin_ups_wgs_LL.xyz
Data Format Option (0-COMCOT; 1-MOST; 2-XYZ)  :    2
```

Figure 4.2: Fault Parameter Section in $COMCOT.CTL$

Fault parameters for a specific earthquake:

No. of FLT Planes (Use fault_multi.ctl if ¡ 1) defines how many fault planes will be implemented to create seafloor deformation. If the number is larger than 1, an additional control file, $FAULT\_MULTI.CTL$ will be required to specify parameters for additional fault planes. The definitions of parameters in $FAULT\_MULTI.CTL$ are the same as this section.

Fault Rupture Time (seconds) defines when this fault plane will rupture. 0.0 means the fault is rupturing at the beginning of the simulation.

Faulting Option (0: Model; 1- Data;) specifies if the seafloor deformation is cre-

ated via fault model (e.g., Okada, 1985) or imported from an external data file. 0 – use fault model with the fault parameters given in this section to calculate seafloor deformation; 1 – use an external data file which contains the seafloor deformation as the initial condition. The file name and format are given in the last two lines of this section.

Focal Depth is the distance measured vertically from the top edge of a fault plane to the mean earth surface.

Length of source area is the length of the rectangular fault plane and **Width of source area** is the width of the rectangular fault plane.

Dislocation of fault plate defines the relative dislocation between foot block and hanging block on the fault plane.

Strike direction defines the strike angle (θ) of the fault plane, measured from the north to the fault line, with the fault plane on the right-hand side.

Dip angle is the angle (δ) between the mean earth surface and the fault plane.

Slip angle is the angle (λ) measured counter clock wise from the fault line to the direction of relative motion of hanging block on the fault plane.

Comp. Domain- Left Edge - Latitude is the latitude of the lower-left (i.e., southeast) corner grid in the 1st-level grid, *layer*01.

Comp. Domain- South Edge - Longitude is the longitude of the lower-left (i.e., southeast) corner grid in the 1st-level grid, layer01.

Epicenter Location: Latitude and **Epicenter Location: Longitude** specify the latitude and longitude of the epicenter of an earthquake.

File Name of Deformation Data specifies the file name of the seafloor deformation data if 1 is chosen at the line **Faulting Option (0: Model; 1- Data;)**. And the data format should be given at the line **Data Format Option (0-COMCOT; 1-MOST; 2-XYZ)**. 3 ASCII formats are supported by COMCOT. 0 – use the old COMCOT format (version1.6 or earlier); 1 – use the MOST format and 2 – use the XYZ format. Latitude of the epicenter of an earthquake.

By default, COMCOT will output the initial condition (initial water surface elevation) in a file named *ini_surface.dat*.

4.1.3   Parameters for Wave Maker

If in the line **Initial Cond. (0:FLT,1:File,2:WM,3:LS,4:FLT+LS)** in General Parameter Section, "2" is selected, parameters for wave maker should be given in the section **Parameters for Wave Maker** in COMCOT.CTL. Either solitary waves or a customized time history profile can be sent into the numerical domain (1st-level grid, layer01) through any of the four boundaries.

```
#====================================================:=============
#   Parameters for Wave Maker                        :Values
#====================================================:=============
 Wave type   ( 1:Solit, 2:given, 3:focusing )    :     1
 FileName of Customized Input (for Type=2)        : fse.dat
 Incident direction( 1:top,2:bt,3:lf,4:rt,5:ob ):     2
 Wave Amplitude                     (meter)   :     0.500
 Typical Water depth                (meter)   :  2000.000
```

Figure 4.3: Wave Maker Parameter Section in $COMCOT.CTL$

Wave type (1: Solitary, 2:given profile) is used to determine the incident wave type: 1 – Send Solitary wave into the numerical domain, layer01; 2 – Input a wave profile defined in a time history file through one boundary whose should be given after

FileName of Customized Input (for Type=2); 3 – generate a focusing solitary wave. When using this option, incident wave through a boundary will converge to a specified location ("focus"). Two additional parameters will be asked for when the program starts: x and y coordinates of the focus in layer01.

Incident direction(1:top,2:bt,3:lf,4:rt,5:ob) defines which boundary the wave is sent through. 1 – waves come from the top boundary of the domain; 2 – waves come from the bottom boundary of the domain; 3 – waves come from the left boundary of the domain; 4 – waves come from the right boundary of the domain; 5 – Oblique incident wave. When using this option, an oblique wave will be sent into the numerical domain through boundaries. The oblique angle will be required after the program starts. The angle ranges is measured from the northward (upward) to the incident direction, ranging from 0.0 to 360..

Characteristic Wave Amplitude specifies the wave amplitude of the incident wave (only effective when solitary wave is sent in).

Typical Water depth specifies the characteristic water depth, which is effective for both wave types. This value is used to calculate volume flux associated with incident waves based on shallow water wave theory.

4.1.4   Parameters for Landslides/Transient Floor Motion

If in the line **Initial Cond. (0:FLT,1:File,2:WM,3:LS,4:FLT+LS)** in General Parameter Section, 3 or 4 is selected, parameters for submarine landslide model (or other submarine transient seafloor motions) should be given in the section **Parameters for Transient Sea Floor Motion** in COMCOT.CTL. Compared to the di-

mension of the simulated region (i.e., layer01), transient seafloor motions (e.g., transient fault rupture, landslides), generally, occur within a small confined area, which is defined by the coordinates of its left (west), right (east), bottom (south) and top (north) margins.

X Coord. of Left/West Edge of Landlide Area specifies X coordinate of grids on the left/west margin of the landslide region.

x Coord. of Right/East Edge of Landlide Area specifies X coordinate of grids on the right/east margin of the landslide region.

Y Coord. of Bottom/South Edge of Landlide Area specifies Y coordinate of grids on the bottom/south margin of the landslide region.

Y Coord. of Top/North Edge of Landlide Area specifies Y coordinate of grids on the top/north margin of the landslide region. It should be noted that the units/coordinates used here should be the same as those of 1st-level grid. For example, if the 1st-level grid, layer01, adopts Spherical Coordinates (Latitude/Longitude), then the values defining the landslide region should also be latitude/longitude in Spherical Coordinates.

File Name of SeaFloor Motion Data specifies the filename of seafloor motion data. This data file contains a time sequence of snapshots of variation of the seafloor relative to its original location.

4.1.5   Parameters for All Grid Levels

Parameters for 1st-Level Grid

In COMCOT.CTL, parameter section for grids of all levels follows the parameter section of landslide model. The section, **Parameters for 1st-level grid – layer 01**, con-

tains configurations for the 1st-level grid (the largest grid region), layer01.

```
#==============================================:==============================
# Configurations for all grids                :Values                        |
#==============================================:==============================
# Parameters for 1st-level grid -- layer 01    :Values                       |
#==============================================:==============================
  Run This Layer ?       (0:Yes,       1:No    ):      0
  Coordinate System    (0:spherical, 1:cartesian):    0
  Governing Equations  (0:linear,    1:nonlinear):    0
  Grid Size  (dx, sph:minute, cart:meter)       :      0.50
  Time step                      ( second )     :      1.0
  Bottom Friction Switch? (0:Yes,1:No,2:var. n ) :     1
  Manning's Roughness Coef. (For fric.option=0)  :     0.013
  Ouput Option? (0: Z+Hu+Hv; 1: Z Only; 2: NONE) :     1
  X_start                                       :  176.0
  X_end                                         :  179.5
  Y_Start                                       :  -40.5
  Y_end                                         :  -36.5
  File Name of Bathymetry Data                  : nz30secv1.bat
  Data Format Option (0-COMCOT;1-MOST;2-XYZ)    :     1
  Grid Identification Number                    :    01
  Grid Level                                    :     1
  Parent Grid's ID Number                       :    -1

#==============================================:==============================
```

Figure 4.4: Parameters for 1st-level grid in *COMCOT.CTL*

The meaning of each entry is illustrated as follows.

Run This Layer? is used to determine if this grid level is included in the numerical simulation. 0 – this grid level will be include; 1 – this grid level will not be included in the simulation.

Coordinate System specifies which coordinates will be used for this grid level. 0 – use Spherical Coordinates; 1 – use Cartesian Coordinates.

Governing Equations determines which type of governing equations will be used for this grid level. 0 – use linear shallow water equations; 1 – use nonlinear shallow water equations. If runup and inundation are going to be calculated, nonlinear shallow water equations must be chosen.

Grid Size specifies the grid size ($\triangle x$) adopted for this grid level. If spherical coordinate system is adopted, the grid size should be given in arc minutes; if cartesian coordinate system is adopted, the grid size should be given in meters.

Time Step determines the time step ($\triangle t$) used for the numerical simulation. The

36

time step chosen should guarantee that Courant condition is satisfied, which means

$$\triangle t < \frac{\triangle x}{\sqrt{gh_{max}}} \tag{4.1}$$

where g is the gravitational acceleration and h_{max} is the maximum water depth within the region of this grid level. If Courant condition is not satisfied for a given time step ($\triangle t$), COMCOT will automatically adjust it to make Courant condition being satisfied. Inside the code, the maximum time step size $\triangle t$ allowed is fixed as $0.5\triangle x/\sqrt{gh_{max}}$.

Bottom Friction Switch? is used to determine if bottom friction is considered in the numerical simulation. 0 – bottom friction will be included and a constant bottom friction coefficient will be applied (Manning's n) and the roughness is given at **Manning's Roughness Coef.**; 1 – bottom friction will not be considered; 2 – bottom friction will be included and variable Manning's roughness coefficient will be applied. The variable roughness coefficients need to be given in a data file named *fric_coef_layerXX.dat* in which *XX* represents the grid ID of this grid level.

Ouput Option? (0: Z+Hu+Hv; 1: Z Only; 2: NONE) is used to control the output of free surface elevation and volume fluxes. 0 – both water surface elevation and volume fluxes (i.e., product of water depth and velocity) will be output; 1 – only water surface elevation not be output. 2 – both water surface elevation and volume fluxes will not be output.

In COMCOT, a grid region (i.e., a rectangular area) is defined by the coordinates of its lower-left /south-west corner (X_Start,Y_Start) and upper-right/north-east corner (X_End,Y_End).

X_Start specifies X coordinate of the left/west margin of the grid region.

X_End specifies X coordinate of the right/east margin of the grid region.

Y_Start specifies Y coordinate of the bottom/south margin of the grid region.

Y_End specifies Y coordinate of the top/north margin of the grid region.

Together with the given grid size, the water depth/land elevation at every grid will be extracted from the input bathymetry/topography data file whose name is given after **File Name of Bathymetry Data**. **File Name of Bathymetry Data** specifies the filename of bathymetry data for this grid level. This data file contains the gridded bathymetric/topographic data for this grid level.

Data Format Option is used to determine which type of data format is adopted for bathymetry data file. 0 – use old COMCOT data format (version 1.6 or earlier); 1 – use MOST format; 2 – use XYZ format (3-column data containing x, y and bathymetry information); 3 – use ETOPO bathymetry data. *XYZ* format is suggested.

Grid Identification Number is used to assign an ID to this grid level. This is the only identification number used to distinguish this grid from the others. It is not suggested to change the value here.

Grid Level is used to determine the level of this grid in the hierarchy of nested grid setup. For the largest grid layer (the 1st level), the grid level is 1.

Parent Grid's ID Number is used to specify which grid layer is the parent grid of this grid layer. The parent grid means the grid layer where the current grid is directly nested in. For the 1st-level grid, the parent grid ID should be specified as -1 (or 0) since it has no parent grid.

Parameters for sub-level grids

The parameter configurations for sub-level grids are very similar to that of the 1st-level grid. But, there is no need to specify the grid size ($\triangle x$) and time step ($\triangle t$) for sub-level grids. However, the grid size ratio of its parent grid to this grid level should be given after **GridSize Ratio of Parent layer to current layer**. The grid size ratio can be any integer larger than or equal to 1. However, a ration less than 10 is suggested.

```
#=======================================================:==================================
#  Parameters for Sub-level grid -- layer 02      :Values                                  |
#=======================================================:==================================
Run This Layer ?        (0:Yes,       1:No     ):     1
Coordinate              (0:spherical, 1:cartesian):    0
Governing Eqn.          (0:linear,    1:nonlinear):    0
Bottom Friction Switch? (0:Yes,1:No,2:var. n ) :      1
Manning's Roughness Coef. (For fric.option=0)  :     0.013
Ouput Option? (0: Z+Hu+Hv; 1: Z Only; 2: NONE) :     1
GridSize Ratio of Parent layer to current layer:     2
X_start                                         : 178.011643
X_end                                           : 178.501284
Y_start                                         : -39.506430
Y_end                                           : -39.025147
FileName of Water depth data                    : depth_nz30sec_LL.xyz
Data Format Option (0-COMCOT;1-MOST;;2-XYZ)     :     2
Grid Identification Number                      :     02
Grid Level                                      :     2
Parent Grid's ID Number                         :     1

#=======================================================:==================================
```

Figure 4.5: Parameters for sub-level grids in *COMCOT.CTL*

In COMCOT, a sub-level grid region (i.e., a rectangular area) is defined by the coordinates of its lower-left /south-west corner (X_Start,Y_Start) and upper-right/north-east corner (X_End,Y_End). This four values should be given in the same coordinates as that used in its parent grid layer. If the current grid layer adopts Cartesian coordinates (UTM) and its parent grid layer adopts Spherical Coordinates (latitude/longitude), then the coordinates of these two corners should be given in laitutde/longitude. In COMCOT, a sub-level grid layer using Cartesian coordinates can be nested inside a grid layer using Spherical coordinates. However, the reverse nesting is not supported.

4.2   Input Data

4.2.1   Bathymetric/Topographical Data

4 ASCII formats of bathymetry data are supported in COMCOT v1.7, the old COMCOT-formatted data (for version 1.6 or earlier), MOST-formatted data and XYZ format data and ETOPO bathymetry data. However, XYZ format is suggested whose format will be detailed here. The bathymetry data file should be in ASCII format and written in 3 columns. The first column contains information of X coordinates (rightward, pointing to the east), and second column contains information of Y coordinates (upward, pointing to the North) and the third column contains the data of water depth (positive for bathymetry data and negative for topographical data), see Figure 4.6.

```
100.0083  24.9926    1485.00
100.0250  24.9926    1381.00
100.0417  24.9926    2063.00
100.0583  24.9926    1923.00
100.0750  24.9926    1403.00
100.0917  24.9926    1439.00
100.1083  24.9926    1369.00
100.1250  24.9926    1351.00
100.1417  24.9926    1453.00
100.1583  24.9926    1385.00
100.1750  24.9926    1289.00
100.1917  24.9926    1405.00
100.2083  24.9926    1577.00
100.2250  24.9926    1547.00
100.2417  24.9926    1865.00
100.2583  24.9926    1773.00
100.2750  24.9926    1923.00
```

Figure 4.6: Example of Bathymetry Data File (XYZ format)

The format of ETOPO data is the same as that of XYZ 3-column data. The only difference is the sign of data. In ETOPO data, the value of water depth is given as a negative number and the land elevation is given as a positive number. The ETOPO

bathymetry data (either ETOPO1 or ETOPO2) can be directly used in COMCOT v1.7. COMCOT will change the sign after the ETOPO data is loaded in.

The bathymetry data must be gridded and the gridded data (a $nx \times ny$ matrix) should be written row by row or column by column from the left/west ($i = 1$) to the right/east ($i = nx$) from the bottom/south ($j = 1$) to the top/north ($j = nx$) where i and j represent the x, y grid index of bathymetry/topography grids and nx and ny are the total number of grids in X and Y direction. The x coordinates must increase monotonically and y coordinates should increase or decrease monotonically. It should be noted that for each grid layer the gridded bathymetry/topography data should adopt the same coordinate system as specified for this grid layer. And the area of bathymetry/topography data should be larger than or equal to the region defined by $X\_S tart$, X_End, $Y\_S tart$ and Y_End in the parameter section for this grid layer.

If a grid layer adopts Cartesian coordinate system, however, its parent grid layer uses Spherical Coordinate system, $X\_S tart$, X_End, $Y\_S tart$ and Y_End of this grid layer should given with spherical coordinates (latitude, longitude). But, the bathymetry data file of this grid layer should be prepared with cartesian coordinates (UTM). The position of this grid layer is determined by $X\_S tart$, X_End, $Y\_S tart$ and Y_End which are given in longitude and latitude. The key to remember is the position of a sub-level grid layer is also defined in the same coordinates as its parent grid layer.

4.2.2 Seafloor Deformation Data

Similar to bathymetry/topography data file, 3 ASCII formats of seafloor deformation data are also supported in COMCOT v1.7, the old COMCOT-formatted data (for version 1.6 or earlier), MOST-formatted data and XYZ format data. However, XYZ format is

also suggested. The seafloor deformation data file should be in ASCII format and written in 3 columns. The format is the same as that of XYZ-format bathymetry data file. The first column contains information of X coordinates (rightward, pointing to the east), and second column contains information of Y coordinates (upward, pointing to the North) and the third column contains the data of water depth (positive for bathymetry data and negative for topographical data), see Figure 4.7.

```
177.000 -37.2   5.91777e-05
177.008 -37.2   4.55538e-05
177.017 -37.2   3.27337e-05
177.025 -37.2   2.40436e-05
177.033 -37.2   5.5204e-06
177.042 -37.2  -1.10822e-05
177.05  -37.2  -1.43968e-05
177.058 -37.2  -4.15083e-05
177.067 -37.2  -5.13296e-05
177.075 -37.2  -6.20628e-05
177.083 -37.2  -9.05449e-05
177.092 -37.2  -9.35145e-05
177.1   -37.2  -0.000112883
177.108 -37.2  -0.000135352
177.117 -37.2  -0.000138304
177.125 -37.2  -0.000172024
177.133 -37.2  -0.000182899
```

Figure 4.7: Example of Seafloor Deformation Data File (XYZ Format)

The deformation data should be gridded and written row by row from the left/west ($i = 1$) to the right/east ($i = nx$) from the bottom/south ($j = 1$) to the top/north ($j = nx$) where i and j represent the x, y grid index of bathymetry/topography grids and nx and ny are the total number of grids in X and Y direction. It should be noted that the deformation data should use the same coordinate system as the 1st-level grid. The area of deformation data should fall inside the region defined by the 1st-level grid.

4.2.3   Transient Sea Floor Motion Data

To generate tsunamis by landslides or any other type of transient seafloor motion, a data file is required to provide information on seafloor motion. This data file contains a sequence of snapshots of seafloor variations in terms of time.

If, for example, the landslide area has a grid dimension of nx and ny where nx and ny stand for the total number of grids in X and Y direction, respectively, and in total, nt snapshots are created to trace the variation of seafloor position in time, the variation of seafloor can be represented as $\triangle h(i, j, k)$, where $i = 1, nx$, $j = 1, ny$ and $k = 1, nt$. $\triangle h(i, j, k)$ describes the variation of the seafloor position against its origin at (i, j) at time level k. And $\triangle h(i, j, k)$ can be obtained from

$$\triangle h(i, j, k) = h(i, j, k) - h0(i, j) \qquad (4.2)$$

in which $h(i, j, k)$ denotes the instantaneous water depth at (i, j) at time level k and $h0(i, j)$ represents the original position of seafloor.

Figure 3.2 gives a simply example of seafloor variation during a landslide event. 3 snapshots are presented to show the positions of seafloor during a landslide event. Snapshot at $t = t0$ shows the original position of sea floor before landslide and snapshots at $t = t1$ and $t = 2$ indicate the intermediate and final stage of seafloor position. Then the variation of seafloor can be described by these 3 snapshots. For example, at $x = x1$, 3 snapshots of seafloor variation are $\triangle h(x1, t0)$, $\triangle h(x1, t1)$ and $\triangle h(x1, t2)$ where $\triangle h(x1, t0) = h(x1, t0) - h(x1, t0)$, $\triangle h(x1, t1) = h(x1, t0) - h(x1, t1)$ and $\triangle h(x1, t2) = h(x1, t0) - h(x1, t2)$, respectively. If $\triangle h > 0$, it indicates that the seafloor is being uplifted; if $\triangle h < 0$, it means the seafloor is being subsided.

After the snapshot data of seafloor variation is determined, the input data file for this transient seafloor motion can be written in the following format. The first line of

43

the data file contains 3 integers specifying the grid dimension, nx and ny, and the total number of snapshots, nt. Then, it follows by the X coordinates of gridded data (from lines 2 to $nx + 1$), Y coordinates of gridded data (from lines $nx + 2$ to $nx + ny + 1$) and the times at which the snapshots are created (from lines $nx + ny + 2$ to $nx + ny + nt + 1$). After the coordinates and time information, it is the section for snapshot data. All the nt snapshots of seafloor variation are written into a single column one by one from $t = t_1$ to $t = t_{nt}$. For each snapshot, e.g., $\triangle h(nx, ny, t_1)$, the data should be written row by row from the left/west ($i = 1$) to the right/east ($i = nx$) from the bottom/south ($j = 1$) to the top/north ($j = nx$) where i and j represent the x, y grid index of gridded snapshot data. It should be noted that the landslide snapshot data should use the same coordinate system as the 1st-level grid. The landslide area should fall inside the region defined by the 1st-level grid. However, the grid and time resolutions are not necessarily the same as those of the 1st-level grid layer. Interpolation will be carried out inside COMCOT. A sample data file is shown in Figure **??**.

```
50 50 50
2.000000
2.030612
2.061224
2.091837
2.122449
2.153061
2.183673
2.214286
2.244898
2.275510
2.306122
2.336735
```

Figure 4.8: Example of Landslide Data File (XYT Format)

Two file formats are supported: the old COMCOT format (for version 1.6) and the new XYT format. The new format is suggested for version 1.7.

4.2.4 Bottom Friction Coefficients

If at the grid parameter section, 2 is chosen after **Bottom Friction Switch?** for one grid layer, a gridded Manning's roughness *n* (varying in space) should be prepared for this grid layer before simulation starts. The roughness coefficient data file has the same format as that of bathymetric/topographical data. The grid size is not necessarily the same as that of the grid layer, but the area covered should be slightly larger than or at least equal to the grid layer. The file name of roughness coefficients should be like *fric_coef_layerXX.dat* in which *XX* represents the grid ID of this grid layer.

4.2.5 Time History Input for Wave Maker

A time history input of water surface elevation is required if the wave maker is implemented and the option **2** is chosen for **Wave type (1: Solitary, 2:given profile)**. The data file should be written in ASCII format and the file name need to be given at the line **FileName of Customized Input (for Type=2)**. The data file contains two data columns. The first column contains the time sequence, $t = t_k$ $(k = 1, \cdots, nt)$, and the second column contains the water surface elevation, $\eta = \eta_k$ $(k = 1, nt)$, corresponding to the time sequence. The units should be *seconds* for time and *meters* for the water surface elevation.

4.2.6 Numerical Tidal Gauge Locations

If in the control file *COMCOT.CTL*, **Output Zmax & TS** is set to 1 or 2, the the time history records will be output at up to 9999 numerical tidal gauge location. A data file, *textbfts_location.dat*, is required to specify these tidal gauge locations. The data file

contains two data columns. The first data column defines the *X* coordinates of tidal gauges and the second column defines the *Y* coordinates of tidal gauges. In Figure 4.9, locations of four tidal gauges are specified.

```
177.15  -36.85
177.77  -37.01
178.34  -38.13
178.12  -29.05
```

Figure 4.9: Example of Tidal Gauge Location File *ts_location.dat*

4.3   Output Data

4.3.1   Time Sequence Data

A data file, named **time.dat**, will always be output for a simulation. The data file contains only one data column, which is the wall-clock time corresponding to each time step during the entire simulation. This output file can be used together with the time history output at specified tidal gauges to create time history plots.

4.3.2   Water Surface Elevation/Volume Fluxes

Generally, only the free surface elevation will be output in data files named in the form *z_ID_xxxxxx.dat*, where *z* stands for free surface elevation, two digits *ID* denote the corresponding grid identification number and the six digits, *xxxxxx*, corresponds to the time step number when the data is output. Therefore, the data file *z_ID_xxxxxx.dat* stores the

free surface elevation at all grid points in the grid layer. For example, $z\_01\_001234.dat$

stores the free surface elevation at all the grid points of $layer01$ at time step 1234. It

should be mentioned that the total number of time steps required for a simulation and

also time step number for data output are also calculated based on the time step ($\triangle t$)

of $layer01$. For example, if $0.5s$ time step is used for $layer01$, the number of time

steps, 1234, corresponds to a physical time $t = 1234 \times 0.5 = 617.0s$. However, if

the switch **Output Volume Flux** is set to 0 for this layer, two additional data files,

$m\_ID\_xxxxxx.dat$ and $n\_ID\_xxxxxx.dat$ will be created, storing volume flux data in x

direction and y direction, respectively, at all the grid points in this grid layer at time step

number $xxxxxx$. The following scripts will be able to read the data in a output data file

"F_AB_dddddd.dat" into a predefined matrix B(nx,ny)

Table 4.1: Fortran scripts to write Water surface/Volume flux data into a data file

```
open (IO-UNIT,file='z_ID_xxxxxx.dat',status='unknown')
do i=1, ny
    read (IO-UNIT, '(15f9.3)') (B(i, j), i=1, nx)
enddo
close(IO-UNIT)
```

In Table4.1, z denotes water surface elevation, for volume flux, z should be replaced

by m for volume flux in X direction or n for volume flux in Y direction; ID represents

Identification Number of a grid layer and $xxxxxx$ stands for the number of time steps

at which the data is written. In addition, if the switch **Output Volume Flux** is set to 2,

neither water surface elevation nor volume fluxes will be out.

To obtain the velocity components (u, v) at a grid, divide the volume flux components

by the total water depth $(\eta + h)$ where η represents the water surface fluctuation.

4.3.3 Initial Condition

At the beginning of a simulation starts, the initial water surface displacement will be written into a data file named *ini_surface.dat*. This data file is written via the following FORTRAN code.

Table 4.2: Fortran scripts to write Initial Condition into a data file

```
open (IO-UNIT,file='ini_surface.dat',status='unknown')
do i=1, ny
    write (IO-UNIT, '(15f8.3)') (deform(i, j), i=1, nx)
enddo
close(IO-UNIT)
```

In Table 4.2, $deform(i, j)$ denotes initial water surface fluctuation at grid (i, j); nx and ny denotes the total number of grids in *X* and *Y* directions, respectively.

4.3.4 Seafloor Deformation

If multiple fault planes are implemented,i.e., in *COMCOT.CTL*, **Initial Cond. (0:FLT,1:File,2:WM,3:I** is set to 0 or 4 and **No. of FLT Planes (Use fault_multi.ctl if ¿1)** is larger than 1, the seafloor deformation generated by each fault plane will be output in data files named *deform_segXX.dat* where *xx* denotes the numbering of fault planes, starting from 01 up to 99. This type of data file is written via the following FORTRAN code.

In Table 4.3, $deform(i, j)$ denotes seafloor deformation at grid (i, j) generated by fault plane *xx*; *nx* and *ny* denotes the total number of grids in *X* and *Y* directions, respectively.

Table 4.3: Fortran scripts to write Seafloor Deformation into a data file

```
open (IO-UNIT,file='deform_segXX.dat',status='unknown')
do i=1, ny
    write (IO-UNIT, '(15f8.3)') (deform(i, j), i=1, nx)
enddo
close(IO-UNIT)
```

4.3.5 Maximum Water Surface Elevation/Depression

If *inCOMCOT.CTL*, **Output Zmax & TS** is set to 0 or 2, the maximum water surface elevation/depression will be output every hour and at the end of a simulation. Every one hour during the simulation, two data files will be created for each grid layer, named **etamax_layerID_XXXXhrs.dat** and **etamin_layerID_XXXXhrs.dat**, in which *ID* denotes the two-digit identification number of each grid layer and the 4-digit *XXXX* represents the number of wall-clock hours elapsing since the tsunami event occurs. The data file **etamax_layerID_XXXXhrs.dat** contains the maximum water surface elevation at every grid for each grid layer included in the simulation in the past *XXXX* hours and **etamin_layerID_XXXXhrs.dat** contains the maximum water surface depression at every grid for each grid layer included in the simulation in the past *XXXX* hours. For example, *etamax_layer01_0001hrs.dat* stores the maximum water surface elevation at all the grid points of *layer*01 within the past 1.0 hours and *etamin_layer01_0001hrs.dat* stores the maximum water surface depression at all the grid points of *layer*01 within the past 1.0 hours. The data file, for example, *etamax_layer01_0001hrs.dat*, is written via the following FORTRAN code.

In Table4.4, η_{max} denotes the maximum water surface elevation of grid layer 01; *nx* and *ny* are the total numbers of grids in *X* and *Y* directions. At the end of the simulation,

Table 4.4: Fortran scripts to write Max/Min Water Surface Fluctuations into a data
file

```
open (IO-UNIT,file='etamax_layer01_0001.dat',status='unknown')

do i=1, ny

    read (IO-UNIT, '(15f9.4)') ($\eta_{max}$(i, j), i=1, nx)

enddo

close(IO-UNIT)
```

two data files, **etamax_layer01.dat** and **etamin_layer01.dat**, will also be created storing the maximum water surface elevation/depression within the entire simulated duration. It should be mentioned that this type of maximum water surface elevation/depression data files will be created for every grid layer included in the numerical simulation.

4.3.6   Time History Records

If in the control file *COMCOT.CTL*, **Output Zmax & TS** is set to 1 or 2, the the time history records will be output at up to 9999 locations given in the data file *ts_location.dat*. A series of data files will be created with the names in the format like *ts_recordxxxx.dat* in which *xxxx* represents the position of a tidal gauge in the data file *ts_location.dat*. For example, if in total 4 tidal gauges are defined in *ts_location.dat*, then four data files, *ts_record001.dat*, *ts_record0002.dat*, *ts_record0003.dat* and *ts_record0004.dat*, will be created corresponding to the four tidal gauges, numbering from top to bottom, in *ts_location.dat*.

4.3.7 Hot Start/Automatic Data Backup

By default, COMCOT will automatically create a resuming snapshot during a simulation for later hot start. The resuming snapshot will be created at the moment specified at **Resuming Time If hot start** in COMCOT.CTL. The simulation can restart from this save snapshot. For this snapshot, three data files will be created which are **z1_layerID_XXXXXX.dat**, **m1_layerID_XXXXXX.dat** and **n1_layerID_XXXXXX.dat**. In the file names, *ID* denotes the 2-digit identification number of a grid layer and *XXXXXX* denotes the corresponding 6-digit time step number. For example, if **Resuming Time If hot start** is set to 1000.0 in a simulation including only one grid layer, 01 and the time step $\triangle t = 1.5$, at time step number $NINT(1000.0/\triangle t) = 667$ ($NINT$ means the nearest integer), the following three data files will be created: **z1_layer01_000667.dat**, **m1_layer01_000667.dat** and **n1_layerlayer01_000667.dat**. The data in these data files are all written in the following format (FORTRAN script) in Table4.5.

Table 4.5: Fortran scripts to write snapshots for hot start

```
open (IO-UNIT,file='F1_layer01_000667.dat',status='unknown')
do i=1, ny
   read (IO-UNIT, '(10f12.5)') (F(i, j), i=1, nx)
enddo
close(IO-UNIT)
```

In Table4.5, *F* denotes one of *z*, *m* and *n*; *nx* and *ny* are the total numbers of grids in *X* and *Y* directions.

This function is designed for a special purpose. In some cases, grid regions of interest are far away from a source region and it will take a long time for the leading wave

of a tsunami to arrive at these regions. The time for the leading wave travelling from the source region to right before entering the small grid regions can be estimated based on water depth and phase speed. Then, this time is specified as the resuming time for a later restart **Resuming Time If hot start** in COMCOT.CTL. At the first step, cold start can be performed with all sub-level grids turned off. After the simulation passes through that specified time, stop the program, modify COMCOT.CTL to turn on all the sub-level grids required, change Start Type to Hot Start and rerun the simulation. For this time, the simulation will start from the specified time with all sub-level grids. Time will be saved. When using the hot start function, if the snapshot data are not there, COMCOT will assume the surface displacements and fluxes everywhere are zeros at that moment and continues the simulation.
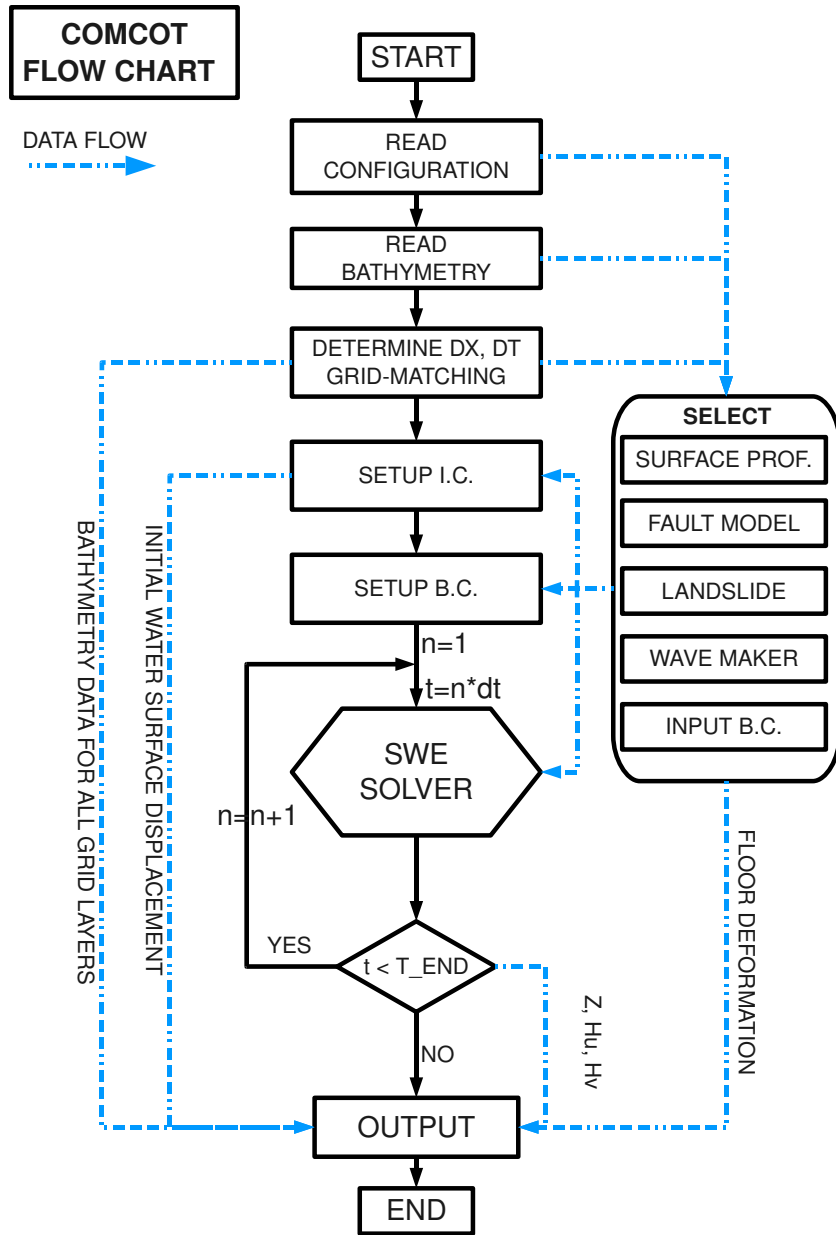
FLOW CHART OF COMCOT

Figure A.1: Flow Chart of COMCOT.

APPENDIX B

OBLIQUE STEREOGRAPHIC PROJECTION

For elastic fault plane theories (e.g., Mansinha and Smylie (1971), Okada (1985)), the displacement is computed over a semi-infinite half plane, special handling is required to map it onto the mean Earth Surface (i.e., Ellipsoidal surface). Oblique Stereographic Projection (Snyder, 1987) is implemented in COMCOT to map the surface of an Ellipsoid (the Earthquake) onto a plane by taking the epicenter as where the plane is tangential to the Earth surface. For this projection in COMCOT, the Earth is described by WGS84 Datum (i.e., semi-major axis $a = 6378137.0m$ and semi-minor axis $b = 6356752.3142m$ with scaling factor $k_0 = 0.9996$). Given the geodetic origin of the projection at the tangent point (φ_0, λ_0), i.e., the latitude and longitude of the epicenter, the parameters defining the conformal sphere are:

$$R = \rho_0 \nu_0 \tag{B.1}$$

$$n = \sqrt{1 + \frac{e^2 \cos^4 \varphi_0}{1 - e^2}} \tag{B.2}$$

$$c = \frac{(n + \sin \varphi_0)(1 - \sin \Phi_0)}{(n - \sin \varphi_0)(1 + \sin \Phi_0)} \tag{B.3}$$

where

$$\rho_0 = \frac{a_0(1 - e^2)}{(1 - e^2 \sin^2 \varphi_0)^{3/2}}$$

$$\nu_0 = \frac{a}{1 - e^2 \sin^2 \varphi_0}$$

$$e = \sqrt{1 - b^2/a^2}$$

$$\sin \Phi = \frac{w_1 - 1}{w_1 + 1}$$

$$w_1 = (S_1 \cdot S_2)^n$$

$$S_1 = \frac{1 + \sin \varphi_0}{1 - \sin \varphi_0}$$

$$S_2 = \frac{1 - e \sin \varphi_0}{1 + e \sin \varphi_0}$$

in which R is the radius of the conformal sphere; e is the eccentricity of the Earth.

The conformal latitude and longitude (Φ_0, Λ_0) of the origin are computed from

$$\Phi_0 = \arcsin\left\{\frac{w_2 - 1}{w_2 + 1}\right\}$$

$$\Lambda_0 = \lambda_0$$

where S_1 and S_2 are as above and $w_2 = c(S_1 \cdot S_2^e)^n = cw_1$.

Then, for any point with geodetic coordinates (φ, λ), the equivalent conformal latitude and longitude (χ, Λ) are computed from

$$\Lambda = n(\lambda - \Lambda_0) + \Lambda_0 \tag{B.4}$$

$$\Phi = \arcsin\left\{\frac{w - 1}{w + 1}\right\} \tag{B.5}$$

where

$$w = c(S_a S_b^e)^n$$

$$S_a = \frac{1 + \sin\varphi}{1 - \sin\varphi}$$

$$S_b = \frac{1 - \sin\varphi}{1 + \sin\varphi}$$

Then for any geodetic location (φ, λ), its projection on the plane tangential to the Earthquake surface at (φ_0, λ_0) can be expressed as

$$x = 2Rk_0 \cos\Phi \sin(\Lambda - \Lambda_0)/\beta \tag{B.6}$$

$$y = 2Rk_0 \left\{\sin\Phi \cos\Phi_0 - \cos\Phi \sin\Phi_0 \cos(\Lambda - \Lambda_0)\right\}/\beta \tag{B.7}$$

in which x and y are two axes of the Cartesian coordinates on the plane with its origin at the tangential point (φ_0, λ_0); x axis points to the north and y axis points to the east and

$$\beta = 1 + \sin\Phi \sin\Phi_0 + \cos\Phi \cos\Phi_0 \cos(\Lambda - \Lambda_0).$$

With the above method, for each location (φ, λ) on the Earth surface (Ellipsoidal surface), it corresponds to a point (x, y) on the plane tangential to the Earth surface at the epicenter (φ_0, λ_0), whose displacement can be computed via either Mansinha and Smylie's method or Okada's approach.

APPENDIX C

MATLAB SCRIPTS FOR DATA PROCESSING

BIBLIOGRAPHY

Y.-S. Cho. *Numerical simulations of tsunami and runup*. PhD thesis, Cornell University, 1995.

F. Imamura, N. Shuto, and C. Goto. Numerical simulation of the transoceanic propagation of tsunamis. *paper presented at the Sixth Congress of the Asian and Pacific Regional Division, Int. Assoc. Hydraul. Res., Kyoto, Japan*, 1988.

K. Kajiura and N. Shuto. Numerical modeling of free-surface flows that are two-dimensional in plan. In *Tsunami in The Sea*, number 9 Part B, pages 395–420. John Wiley and Sons, Inc., 1990.

J.F. Lander and P.A. Lockridge. *United States Tsunamis*. U.S. Department of Commerce, 1989.

P. L.-F. Liu, Y.-S. Cho, S. B. Yoon, and S. N. Seo. Numerical simulations of the 1960 chilean tsunami propagation and inundation at hilo, hawaii. In *Recent Development in Tsunami Research*, pages 99–115. Kluwer Academic Publishers, 1994.

P. L.-F. Liu, S-B. Woo, and Y-S Cho. Computer programs for tsunami propagation and inundation. Technical report, Cornell University, 1998.

P.L.-F. Liu, Y-S. Cho, M.J. Briggs, C.E. Synolakis, and U. Kanoglu. Run-up of solitary waves on a circular island. *J. Fluid Mech*, 302:259–285, 1995.

L. Mansinha and D. E. Smylie. The displacement fields of inclined faults. *Bull. Seism. Soc. Am.*, 61:1433–1440, 1971.

M. Okada. Surface deformation due to shear and tensile faults in a half-space. *Bull. Seism. Soc. Am.*, 75(4):1135–1154, 1985.

N. Shuto. Numerical simulation of tsunamis - its present and near future. *Natural Hazards*, 4:171–191, 1991.

J. P. Snyder. Map projects - a working manual. *U.S. Geological Survey Professional Paper 1395*, page 383, 1987.

X. Wang. *Numerical modelling of surface and internal waves over shallow and intermediate water*. PhD thesis, Cornell University, 2008.

X. Wang and P. L.-F. Liu. A numerical investigation of boumerdes-zemmouri (algeria) earthquake and tsunami. *CMES*, 10(2):171–184, 2005.

X. Wang and P. L.-F. Liu. An analysis of 2004 sumatra earthquake fault plane mechanisms and indian ocean tsunami. *J. Hydraulic Res.*, 44(2):147–154, 2006.

X. Wang and P. L.-F. Liu. Numerical simulations of the 2004 indian ocean tsunamis - coastal effects. *Journal of Earthquake and Tsunami*, 1(3):273–297, 2007.

S. B. Yoon. Propagation of distant tsunamis over slowly varying topography. *J. Geophys. Res.*, 101(C10):3140–, 2002.